

M41
H43
no.49
[redacted]

NATURAL CONVECTION FLOWS IN
PARALLEL CONNECTED VERTICAL
CHANNELS WITH BOILING

MASS. INST. TECH.
SEP 13 1967
LIBRARY

Peter W. Eselgroth
Peter Griffith

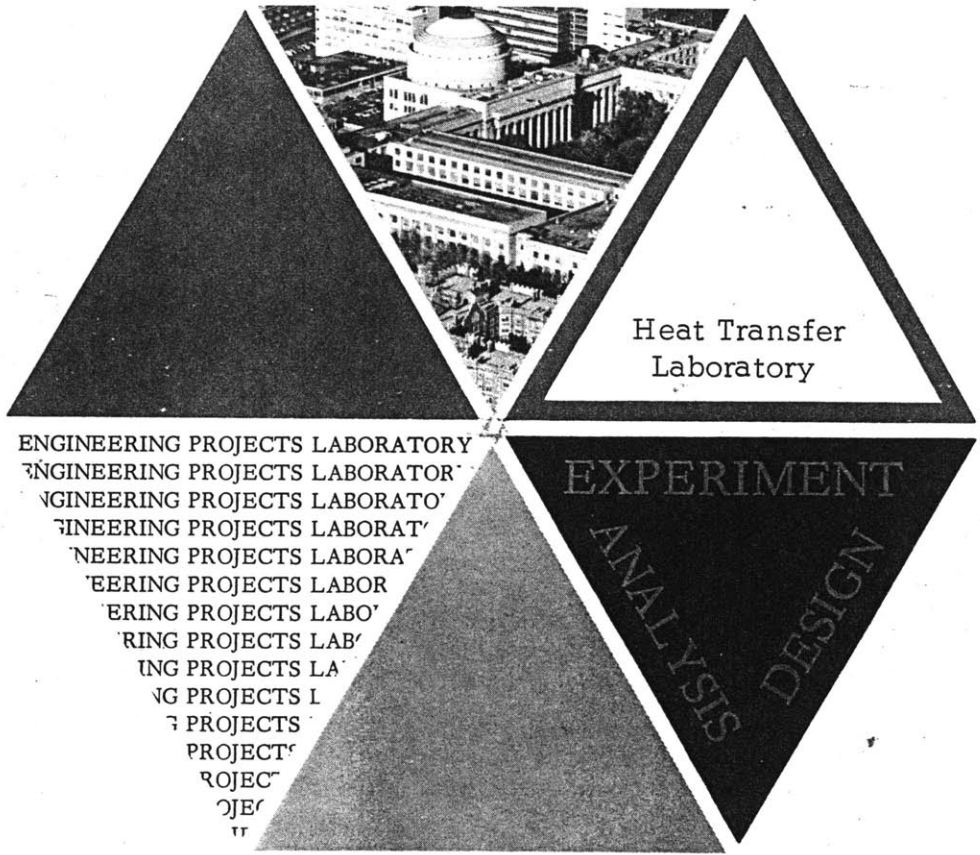
Report No. 70318 - 49

MASS. INST. OF TECHNOLOGY
JAN 22 1968
ENGINEERING LIBRARY

Contract No. AT(30-1)-3496

Department of Mechanical
Engineering
Engineering Projects Laboratory
Massachusetts Institute of
Technology

July 1967



NATURAL CONVECTION FLOWS IN PARALLEL CONNECTED
VERTICAL CHANNELS WITH BOILING

by

Peter W. Eselgroth
Peter Griffith

Sponsored by the Atomic Energy Commission
Contract No. AT(30-1)3496

July 1967

Department of Mechanical Engineering
Massachusetts Institute of Technology
Cambridge, Massachusetts
02139

ABSTRACT

The steady-state flow configuration in an array of parallel heated channels is examined with the objective of predicting the behavior of a reactor during a loss of flow accident. A method of combining the results of single tube experiments with a calculation scheme for the multiple tube array is developed. Only single -single tube experiments were run.

These are three possible flow solutions for a channel. They are as follows: gas and liquid flowing up, gas flowing up and liquid down, and both gas and liquid flowing down. This investigation eliminates the latter as a possible solution for a channel operating in an array of channels. For the two remaining flow cases the constraints of a common pressure drop across the channels and the satisfaction of continuity in the closed end plenum, determine a solution for each heat flux distribution over the array.

The data in this investigation was obtained using Freon 113 as the coolant for an electrically heated glass tube. The data presented is not intended for use other than verification of the method of solution proposed. It is recommended that the coolant intended for use in the application be used with a prototype, rather than a model, channel in obtaining the single channel data.

TABLE OF CONTENTS

ABSTRACT	ii
LIST OF FIGURES	iv
1. INTRODUCTION	1
1.1. Background of Problem	1
1.2. Approach to Problem	1
2. ANALYTICAL CONSIDERATIONS	5
2.1. Two-Phase Pressure Drop	5
2.2. Single and Multiple Channel Behavior	6
2.3. Single Channel Dynamics	7
2.4. The Pressure Drop Versus Flow Rate Curve	10
2.5. The Pressure Drop Versus Heat Flux Map	12
3. EXPERIMENTAL PROGRAM	14
3.1. Purpose of Experimental Program	14
3.2. Description of Apparatus	14
3.3. Experimental Procedure	21
4. RESULTS AND DISCUSSION	22
4.1. Pressure Drop Versus Heat Flux Map	22
4.2. Flow Regimes and Photographs	22
4.3. Pressure Drop Versus Velocity Map	35
4.4. Exclusion of Gas and Liquid Flowing Down	36
4.5. Analytical Predictions	38
5. CONCLUSIONS	40
APPENDIX A. STABILITY ANALYSIS	41
APPENDIX B. VOID FRACTION	45
APPENDIX C. PRESSURE DROP ANALYSIS	47
APPENDIX D. BURNOUT ANALYSIS	56
APPENDIX E. TEST SECTION SPECIFICATIONS	59
APPENDIX F. SOME PHYSICAL PROPERTIES	60
BIBLIOGRAPHY	61

LIST OF FIGURES

1.	Heat Flux and Pressure Drop Decay Curves	3
2.	Pressure Drop Versus Flow Rate Curve	11
3.	Pressure Drop Versus Flow Rate Curve	12
4.	Pressure Drop Versus Heat Flux Curve	13
5.	Test Set-Up: Gas and Liquid Flowing Up	15
6.	Test Set-Up: Gas Flowing Up and Liquid Flowing Down	16
7.	Test Set-Up: Gas and Liquid Flowing Down	17
8.	Relationship of Channel Heated and Unheated Sections, Part a (Figs. 1 and 2) Part b (Fig. 3)	20
9.	Pressure Drop Ratio Versus Heat Flux; The length (L) includes the unheated and heated channel sections	23
	* - burnout	
	[- curve terminated due to nucleation instability	
	o - gas up - liquid up data pt.	
	□ - gas up - liquid down data pt.	
	Δ - zero liquid flow line (i. e., $V_{fs} = 0$)	
	V_{fs} - superficial entering liquid velocity, Q_f/A	
10.	Flow Regime Map; the regime identified was the one uppermost in the channel	24
11.	Pressure drop ratio versus Velocity: Gas and Liquid Flowing Down; V_{fs} , superficial entering liquid velocity, Q_f/A	25
	◇ $q/Aw = 2,000$ BTU/hr-ft. ²	
	▽ $q/Aw = 3,000$	
	□ $q/Aw = 4,000$	
	△ $q/Aw = 5,000$	
12.	Pressure Drop Ratio Versus Velocity: All Three Flow Cases	26
13.	Pressure Drop Ratio Versus Heat Flux: Comparison of Experimental Data with Calculations	27
14.	Calculated Gravity and Friction Pressure Drop Contributions	28
15.	Pressure Drop Ratio Versus Velocity: Comparison of Experimental Data with Calculations	29

LIST OF FIGURES (Continued)

16.	Photographs: Slug-Annular; Slug-Annular Incipient Burnout; Burnout	30
17.	Photographs: Counter Current Annular; Counter Current Annular with Interface, Burnout	31
18.	Photographs: Slug: Cocurrent Annular; Bubbly, Gas and Liquid Down; Gas and Liquid Down, Incipient Gas Reversal	32
19.	Channel Characteristic Operating Curve	36

NOMENCLATURE

A	area, cross-sectional, ft. ²
C	specific heat at constant pressure, BTU/lbm-F ^o
D	channel diameter, ft.
f	friction factor
g	acceleration of gravity, ft/sec. ²
h	enthalpy, BTU/lbm
h _z	height, ft.
I(=ρL/A)	fluid element inertia, lbm/ft. ⁴
K	gravity coefficient, lbf-hr/ft. ⁵
L	channel length (over-all), ft.
M	mass, lbm
n	number of channels
P	pressure, lbf/in. ²
Q(=W/ρ)	volume flow rate, ft. ³ /hr
\bar{Q}	defined in Sec. 2.4
q	heat transfer rate, BTU/hr
R	friction coefficient, lbf-hr/ft. ⁵
S	control volume surface area, ft. ²
T	temperature, °F
t	time, sec., hr.
V	velocity, ft./sec.
V*	dimensionless velocity
$\bar{V}(=\bar{Q}/A)$	velocity defined by \bar{Q}/A , ft./sec.
v	specific volume, ft. ³ /lbm
X = $\frac{W_g}{(W_f + W_g)}$	flowing mass quality

Subscripts

a	annulus
b	bulk
c	held constant
f	liquid
g	gas
i	initial

NOMENCLATURE (Continued)

Subscripts

L	lower plenum
o	final, out, arbitrary time (t_o)
s	superficial
U	upper plenum
W	wall
z	denotes height
1(L_1)	lower unheated section
2(L_2)	heated section
3(L_3)	upper unheated section
in	condition at inlet to channel
out	condition at outlet of channel

Greek Letters

$\alpha \left[= A_g / (A_f + A_g) \right]$	local void fraction
Δ	denotes difference or small change
ρ	mass density, lbm/ft.^3
$\tau \left[= I / (R + K) \right]$	time constant, sec., hr.

1. INTRODUCTION

1.1. Background of Problem

During a "loss of flow" accident in a nuclear reactor the heat flux (q/A_w) at any point in the reactor core and the pressure drop across it are decreasing functions of time. For normal operation the dimensionless pressure drop ratio, $\Delta P_{L,U}/\rho_f g L$, has a value of approximately four. During normal operation of a pressurized-water reactor liquid flows upward in all of the coolant channels. For a boiling-water reactor, gas and liquid flow up in each channel of the reactor core. However, during a "loss of flow" accident when the pressure drop ratio decreases into the neighborhood of one the flow behavior for a single channel could be any of three possibilities. They are, gas and liquid flowing up, gas flowing up and liquid down, and gas and liquid flowing down.

When a nuclear reactor is designed, one of the considerations is that none of the channel walls be permitted to reach, during normal operation, temperatures high enough to cause burnout. The high temperatures which result in this over heating of the channel wall are a result of a localized deficiency in the heat transfer coefficient. Hence, a good deal of theoretical and experimental work has been done so as to avert this problem for normal and abnormal operating conditions. However, it is believed that the possibility of burnout during a "loss of flow" accident has not generally been completely explored. In this study it was desired to develop a method for predicting performance in this region. This method should be one which could be utilized during the design of a reactor so as to avoid this problem.

1.2. Approach to Problem

In a nuclear reactor the pressure drop across the core, at a particular time during a "loss of flow" accident, is common to all channels. The imposed heat flux on the channels decreases with radius from the center of the core. In this analysis the assumption is made that the height to diameter ratio of the core is large enough so that the heat flux is only a function of radius in the horizontal plane. Therefore, at a given time the heat flux is approximately constant over the length of a particular channel.

For purposes of illustrating these facts, sketches of a simplified core configuration and decay curves are shown in Fig. 1.

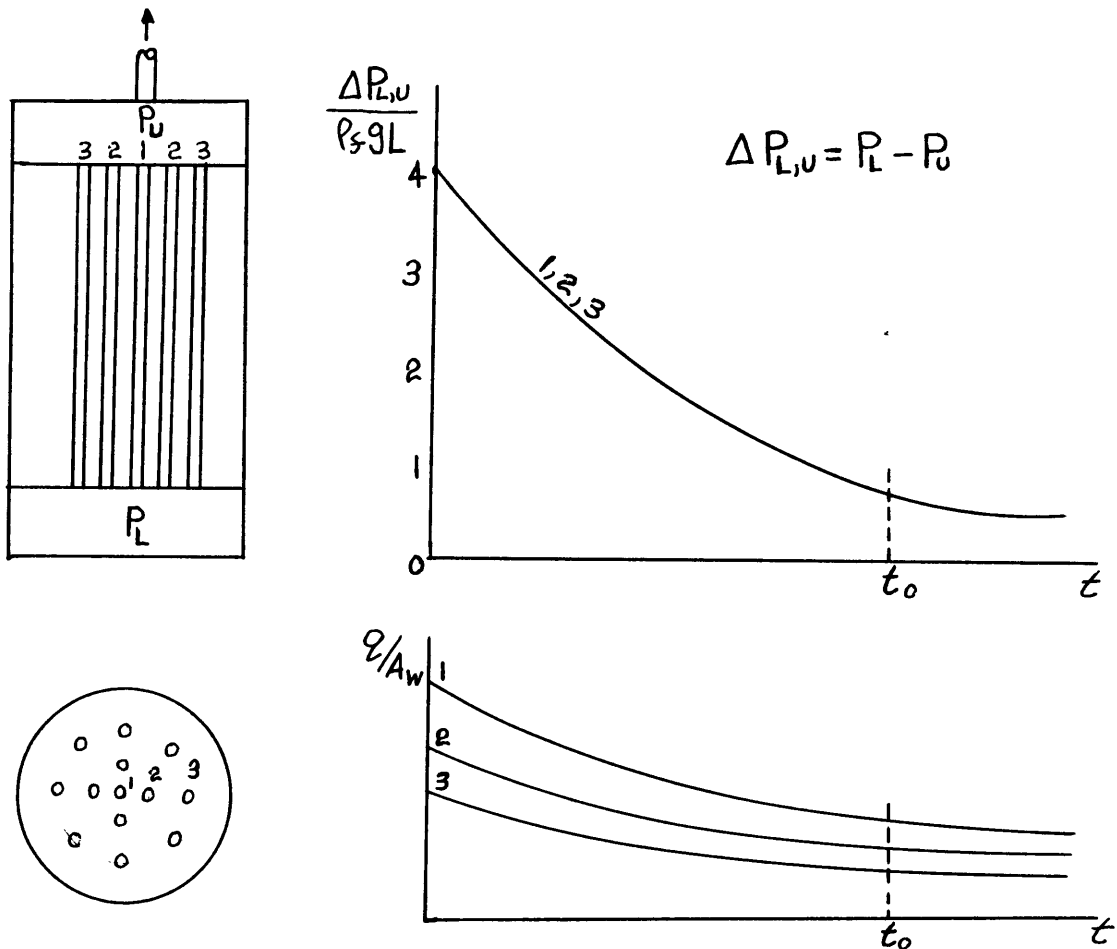


Figure 1

A coolant entrance to the lower plenum is not indicated since, for studies of "loss of flow" accidents the coolant entrance to the reactor is considered to be closed off while the exit is not.

Since the material, diameter and length of all the channels is the same, the results of experimentation with a single channel would apply to each of the channels in the array as long as the proper individual conditions are used. For a given time (t_0) the pressure drop is the same for each channel and the only variable is the heat flux. However, a difficulty in this approach is the possibility that the flow in one or more of the channels may be that of gas and liquid flowing down. The question then is what happens to this gas. It is quite reasonable to assume that most, if not all, of the gas would proceed to the upper plenum through entirely random channels. The randomness with which this would occur would preclude the use of single channel experiments for predicting what was happening in any of the

channels. However, it will be shown later that the case of gas and liquid flowing down will not occur in a channel which operates in an array of channels.

With the possibility of gas and liquid flowing down excluded, the avenue of approach previously outlined may be continued. A map could be constructed from the single channel data using coordinates of pressure drop versus heat flux. This map would include three distinct regions, gas and liquid up, gas up-liquid down, and a region of burnout. If, during the single channel experiments, the liquid flow rate - entering the channel for the case of gas and liquid up and exiting from it when the liquid is flowing down - were held constant, then lines of constant liquid flow rate could also be placed on the map. At a given time (t_0) the heat flux for each channel in the array may be found from the predicted heat flux decay curves. The intersections of vertical lines drawn on the map to represent the channel heat fluxes with a horizontal pressure drop line establishes a possible operating point at time (t_0). Whether or not this is an operating point for the array of channels depends on the satisfaction of continuity in the liquid filled lower plenum. Each intersection of the horizontal line with the vertical lines establishes a liquid flow rate into or out of the plenum for each channel from which continuity may be checked. This method may be used to check the proximity of the channels in the array to the burnout region, for each operating point. Alterations in the design could then be instigated if any of the channels were found to pass too close to or into the burnout region. This is the solution to the stated problem. The investigation is centered around delineating the regions and flow lines on the pressure drop versus heat flux map and the exclusion of gas and liquid flowing down as a possibility.

2. ANALYTICAL CONSIDERATIONS

2.1. Two-Phase Pressure Drop

For two-phase flow the pressure drop is generally separated into the acceleration, friction and gravity contributions. This becomes,

$$\Delta P = (\Delta P)_{\text{acc.}} + (\Delta P)_{\text{fric.}} + (\Delta P)_{\text{grav.}} \quad (1)$$

For normal boiling-water reactor operation where

$$\frac{\Delta P}{\rho_f g L} \cong 4 \quad (2)$$

the gravity contribution is small and therefore,

$$\Delta P \cong (\Delta P)_{\text{acc.}} + (\Delta P)_{\text{fric.}} \quad (3)$$

However, for this investigation where

$$0 \leq \frac{\Delta P}{\rho_f g L} \leq 1 \quad (4)$$

the acceleration contribution has been shown in Appendix C, using a homogeneous model, to be negligibly small. Therefore, in this region

$$\Delta P \cong (\Delta P)_{\text{fric.}} + (\Delta P)_{\text{grav.}} \quad (5)$$

A further simplification can be made when the liquid velocity entering the channel is less than one foot per second. Since the friction pressure drop is a function of the velocity squared, it would be expected that for these small entering liquid velocities, $(\Delta P)_{\text{fric.}}$ would be negligible. This assumes that the heat flux and length of the channel are below certain values such that the acceleration of the liquid by the gas phase is not great enough

to change this. An investigation by Govier, Radford and Dunn (1⁺) presents data for air-water mixtures which shows the friction pressure drop to be small under similar conditions. Further information on this investigation is given in Appendix C.

Therefore, it is assumed that for entering liquid velocities less than one foot per second,

$$\Delta P \cong (\Delta P)_{\text{grav.}} \quad (6)$$

Regions defined by Eq. (6) will be referred to as "gravity dominated", and those where

$$\Delta P \cong (\Delta P)_{\text{fric.}} \quad (7)$$

as "friction dominated".

2.2. Single and Multiple Channel Behavior

In single channel experiments, the pressure drop over the channel length is dependent upon the heat flux and the flow rate through it. In a study of system-induced instabilities by Maulbetsch and Griffith, (2), the following argument is given to show that for an array of channels the pressure drop across any individual channel is independent of the flow through it. The case considered is that of flow passing from one header to another through "n" identical channels. Therefore, the flow rate is distributed uniformly among the "n" channels, each channel carrying "1/n" of the total flow, and the pressure drop is common to all of the channels in the array. If one channel were to become totally blocked, each of the remaining channels would then carry 1/n-1 of the total flow. As "n" becomes large,

$$\frac{1}{n} \approx \frac{1}{n-1} \quad (8)$$

and the change in the pressure drop across the array is negligible. Hence, it is argued that the pressure drop across a channel operating in an array of channels is independent of the flow within it. For the problem considered in this investigation the flow rates, on account of the variation in the channel heat fluxes, may vary from channel to channel. However, the result of a

⁺The numbers in parentheses refer to the references in the Bibliography listed on page 61.

channel operating in an array of channels is seen to carry over into this case of nonuniform flows.

2.3. Single Channel Dynamics

An important part of the method of solution proposed is the application of data taken with flow rate as the independent variable and pressure drop as the dependent variable, to the reverse situation. That is, to the multiple channel case where pressure drop is the independent variable and flow rate is the dependent variable. In either case the heat flux is regarded simply as a parameter. The independent and dependent variable classifications are assigned in the following manner. In the single channel experiments the flow rate is to be varied (independent variable), and the resulting corresponding pressure drop (dependent variable) over a range of heat fluxes, is recorded. For the array of channels, the problem becomes one of imposing a pressure drop (independent variable) on the array and determining the resultant flow rate (dependent variable) in each channel for the various heat fluxes (parameter).

In the single channel experiments, data for all three flow cases may be obtained. In the Introduction it was stated that the case of gas and liquid flowing down will not occur in a channel which operates in an array of channels. If a portion of this flow case is "gravity dominated" then for this portion the flow is an unstable mode of operation for a channel in an array of channels. While the "friction dominated" region is stable. The question of interest now is why the case of gas and liquid flowing down is unstable for a channel in an array, but a stable mode of operation in the single channel experiments. In Sec. 2.2, it was shown that in an array of channels the pressure drop across an individual channel, supplied by the external system (i. e., the plenum to plenum pressure drop), is independent of the flow within the channel. This means that if a flow perturbation occurs in an individual channel, the external system pressure drop remains the same. A stable mode of operation, gas and liquid flowing up in a channel, is considered first. The initial conditions are that the flow passing through the control volume, defined by the channel wall and ends, is in force equilibrium and that the pressure drop through the channel is "gravity dominated". Also, the heat flux is constant. If the flow in the channel experiences an upward perturbation in the entering liquid velocity, the gravity force on the control volume will increase. This is due to the decrease in the void fraction (α) caused by the perturbation. The pressure drop imposed by the external

system is unchanged by the flow perturbation, as previously discussed, and the result is an unbalanced force on the control volume which opposes the flow perturbation. If the flow perturbation were a decrease in the flow rate, the resultant increase in the void fraction causes the gravity force to decrease and the net force on the control volume would be upward. Here again the force imbalance opposes the flow perturbation. Therefore, for gas and liquid flowing up in the "gravity dominated" region, the restoring force is positive and the flow is in stable equilibrium. The same is true in the "friction dominated" region.

However, consider now the case of gas and liquid flowing down with the same initial conditions. A flow perturbation, regardless of its direction, will always produce an unbalanced force on the control volume which aids the perturbation (i. e., a negative restoring force). The equilibrium is, therefore, unstable.

Two distinct differences exist, with regard to this instability, between the single channel experiments and the channel operating in an array of channels. One is that in the single channel experiments the pressure drop imposed by the external system and that which exists through the channel are always identical and not independent of the flow rate. The other difference is that in the single channel experiments the entering liquid flow rate is held constant, although small perturbations do exist due to the unsteadiness of two-phase flow in the channel. However, the flow is constrained from changing beyond small fluctuations. This constraint on the flow prevents the over-all mass of fluid in the channel from being accelerated. This acceleration is not to be confused with that which occurs as a function of length in the heated channel due to vaporization of the liquid.

A more rigorous approach to the stability analysis of gas and liquid flowing down is presented in Appendix A. In this simplified analysis a linearized differential equation,

$$\Delta P_{L,U} = I \frac{dQ_{in}}{dt} + RQ_{in} + KQ_{in} + B \quad (9)$$

was derived which represents the dynamic behavior of the three flow cases. The first, second and third terms on the right-hand side of this equation represent the inertia, friction and gravity contributions to the pressure drop,

respectively. Q_{in} is the liquid volume flow rate entering the channel.

For analyzing the behavior of a channel in an array of channels,

$$\Delta P_{L,U} = \left[\Delta P_{L,U} \right]_c \quad (10)$$

a constant throughout the duration of a flow perturbation. Before a perturbation in the flow rate is introduced

$$\frac{dQ_{in}}{dt} = 0 \quad (11)$$

and Eq. (9) reduces to

$$\frac{\left[\Delta P_{L,U} \right]_c - B}{(R + K)} = Q_{in} \quad (12)$$

This equation defines $(Q_{in})_i$, the initial flow rate at time zero. A perturbation in the flow rate is introduced at time zero plus. This is represented by a step input of ΔQ_{in} , such that

$$Q_{in}(0^+) = (Q_{in})_i + \Delta Q_{in} \quad (13)$$

For these conditions, the solution to the differential equation is

$$Q_{in}(t) = (Q_{in})_i + \Delta Q_{in} e^{-t/\tau} \quad (14)$$

where

$$\tau = \frac{I}{R + K} \quad (15)$$

The stability criterion, therefore, is

$$\tau > 0 \quad (16)$$

The inertance I, $(\rho L/A)$, is always positive, hence the criterion for stability becomes

$$R + K > 0 \quad (17)$$

Since

$$\frac{dQ_{in}}{dt} = 0 \quad (11)$$

in the single channel experiments, Eq. (9) reduces to

$$\Delta P_{L,U} = (R + K) Q_{in} + B \quad (18)$$

or

$$\frac{d(\Delta P_{L,U})}{dQ_{in}} = (R + K) \quad (19)$$

It is apparent that, for a given flow case, the slope of the pressure drop versus flow rate curve from the single channel experiments, for constant heat flux, determines the stability for operation in an array of channels.

2.4. The Pressure Drop Versus Flow Rate Curve

If for the case of gas and liquid flowing down a "friction dominated" region and a "gravity dominated" region are assumed to exist, a sketch of $\Delta P_{L,U}$ versus Q_{in} for constant q/Aw would be expected to appear as shown in Fig. 2.

The flow rate \bar{Q}_{in} is the downward flow rate which neither forces the gas down the channel nor permits it to rise. The pressure drop through the channel would become zero as the gas, being continually generated, filled the channel. Considering the abscissa of the above diagram, it is apparent that the gas rises in the channel for $Q_{in} > \bar{Q}_{in}$ and is forced down when $Q_{in} < \bar{Q}_{in}$. The pressure drop in the gravity dominated region may be expressed as

$$\Delta P_{L,U} = (1 - \alpha_{avg.}) \rho_f g L \quad (20)$$

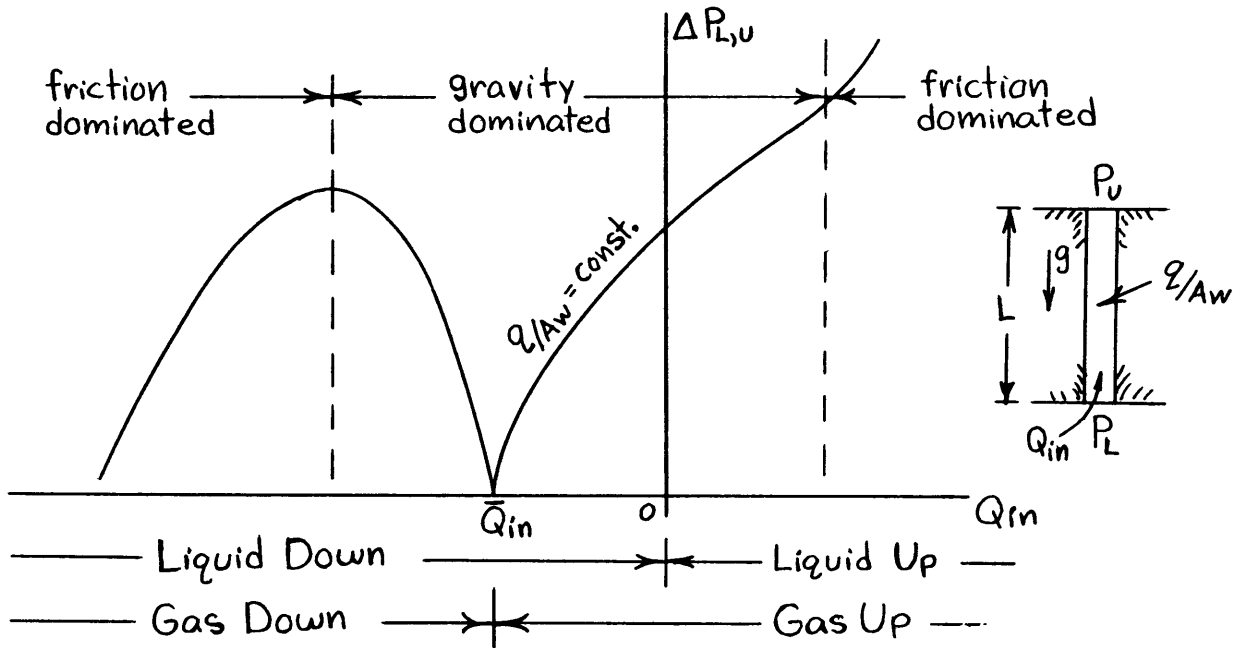


Figure 2

where α_{avg} is the average void fraction. As the flow rate (Q_{in}) is decreased from \bar{Q}_{in} (i.e., as the downward liquid flow rate increases), the average void fraction decreases and in the gravity dominated region $\Delta P_{L,U}$ increases. However, $\Delta P_{L,U}$ begins to decrease as the flow enters the friction dominated region.

For the case of gas up and liquid down ($\bar{Q}_{in} < Q_{in} < 0$), $\Delta P_{L,U}$ would be expected to increase as the down flow of liquid is decreased. This decrease in the liquid flow rate permits the gas to rise faster which causes the average void fraction in the channel to decrease. Therefore, $\Delta P_{L,U}$ would increase as $|Q_{in}|$ decreased in this region.

In the gravity dominated region of gas and liquid flowing up, the average void fraction decreases as Q_{in} increases, and the pressure drop ($\Delta P_{L,U}$), therefore, increases. When the flow enters the friction dominated region, $\Delta P_{L,U}$ continues to increase as Q_{in} is increased, but more rapidly.

In Sec. 2.3, it was shown that in a region in which the slope of the pressure drop flow rate curve was negative, the operation of a channel in an array would be unstable. Figure 2 indicates that the case of gas and liquid flowing down when the flow is gravity dominated, is such a region. The existence of this region (i.e., a portion of the $\Delta P_{L,U}$ versus Q_{in} curve having a negative slope) depends on whether \bar{Q}_{in} is in the gravity or the friction dominated region. If \bar{Q}_{in} were in the friction dominated region, the general shape of the curve would be as shown in Fig. 3.

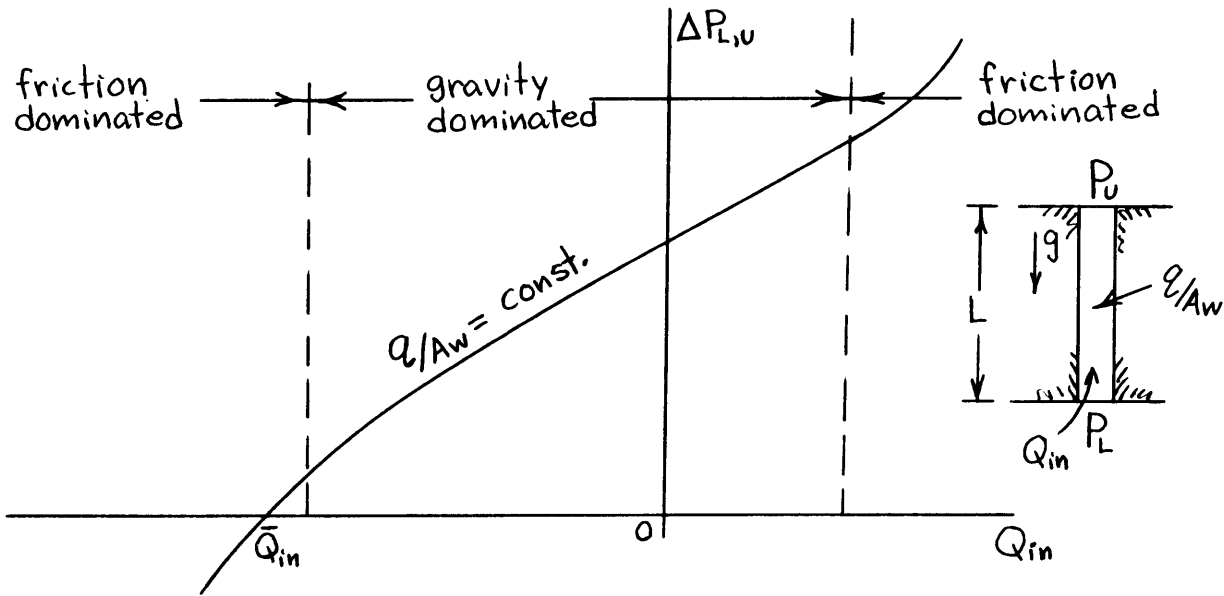


Figure 3

Which general shape the $\Delta P_{L,U}$ versus Q_{in} curve will be, as indicated by Figs. 2 and 3, must be determined experimentally. However, an estimate of the value of \bar{Q}_{in} or $V_{fs}(\bar{Q}_{in}/A)$ may be obtained as shown in Appendix B. An approximation as to when the down flow will become friction dominated may also be calculated.

2.5. The Pressure Drop Versus Heat Flux Map

The pressure drop versus heat flux map would consist, as previously discussed, of three regions: gas and liquid up, gas up-liquid down, and burnout. The general shape of the map would be expected to appear as shown in Fig. 4.

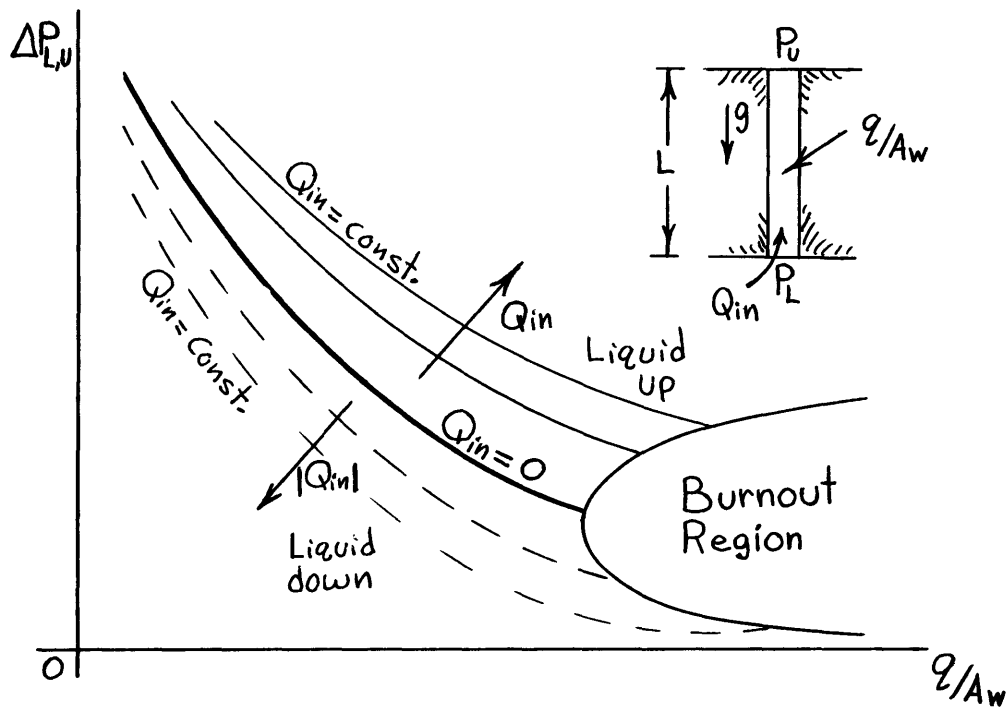


Figure 4

When the liquid flow rate entering the channel is zero, a heated channel with the bottom end closed off, the average void fraction will increase as the heat flux (q/A_w) is increased. Therefore, the pressure drop will decrease as the heat flux increases. This is shown as the $Q_{in} = 0$ line in Fig. 4.

The pressure drop versus heat flux map, as discussed in Sec. 1.2, was to be developed from the single channel experiments for constant entering liquid flow rate. Lines of constant entering Q_{in} are shown in Fig. 4, and the directions of increasing flow rate may be determined from Figs. 2 or 3. Burnout in each of the two flow regions would be expected to occur at higher heat fluxes as the absolute value of the flow rate increased, as shown in Fig. 4.

3. EXPERIMENTAL PROGRAM

3.1. Purpose of Experimental Program

The experimental portion of the investigation consisted of obtaining single channel data for the three flow conditions, gas up-liquid up, gas up-liquid down, and gas down-liquid down. The objective of this program was to verify the expected layout of the pressure drop versus heat flux map and the elimination of the case of gas and liquid flowing down as a possibility in an array of channels.

3.2. Description of Apparatus

In obtaining data for each of the three flow possibilities, the same components of a single apparatus were used and simply relocated to conform to the requirements of the particular flow case being tested. Schematics of the test set-up for gas up-liquid up, gas up-liquid down, and gas down-liquid down are shown in Figs. 5, 6, and 7 respectively. For convenience, the apparatus description has been separated into two categories: the hydraulic system and the instrumentation and auxiliary equipment.

Freon 113, a DuPont product, was chosen as the coolant primarily for its low boiling point. The physical properties of Freon 113, important to this investigation, are presented in Appendix F.

3.2.1. Hydraulic System

A tin oxide coated glass tube, produced by Corning Glassware, was used as the single channel test section. This thin external metallic coating permitted both electrical heating of the glass tube and visual observation of the flow within it. Physical measurements and specifications of this tube are given in Appendix E. A plastic compression type fitting, with a teflon farle insert, was used in connecting the glass test section to the system - in each test set-up.

An Ingersoll Rand Cameron Pump with a teflon packing was used to circulate the Freon 113. In Fig. 5, the pump output was used to force the Freon up through the test section, as well as to maintain the liquid level in the condenser. For the case of gas up-liquid down, Fig. 6, the lower end of the test section was connected to the input of the pump so as to draw liquid from the condenser down through the test section. The pump output was used to replenish the pool of liquid in the condenser and maintain the liquid level.

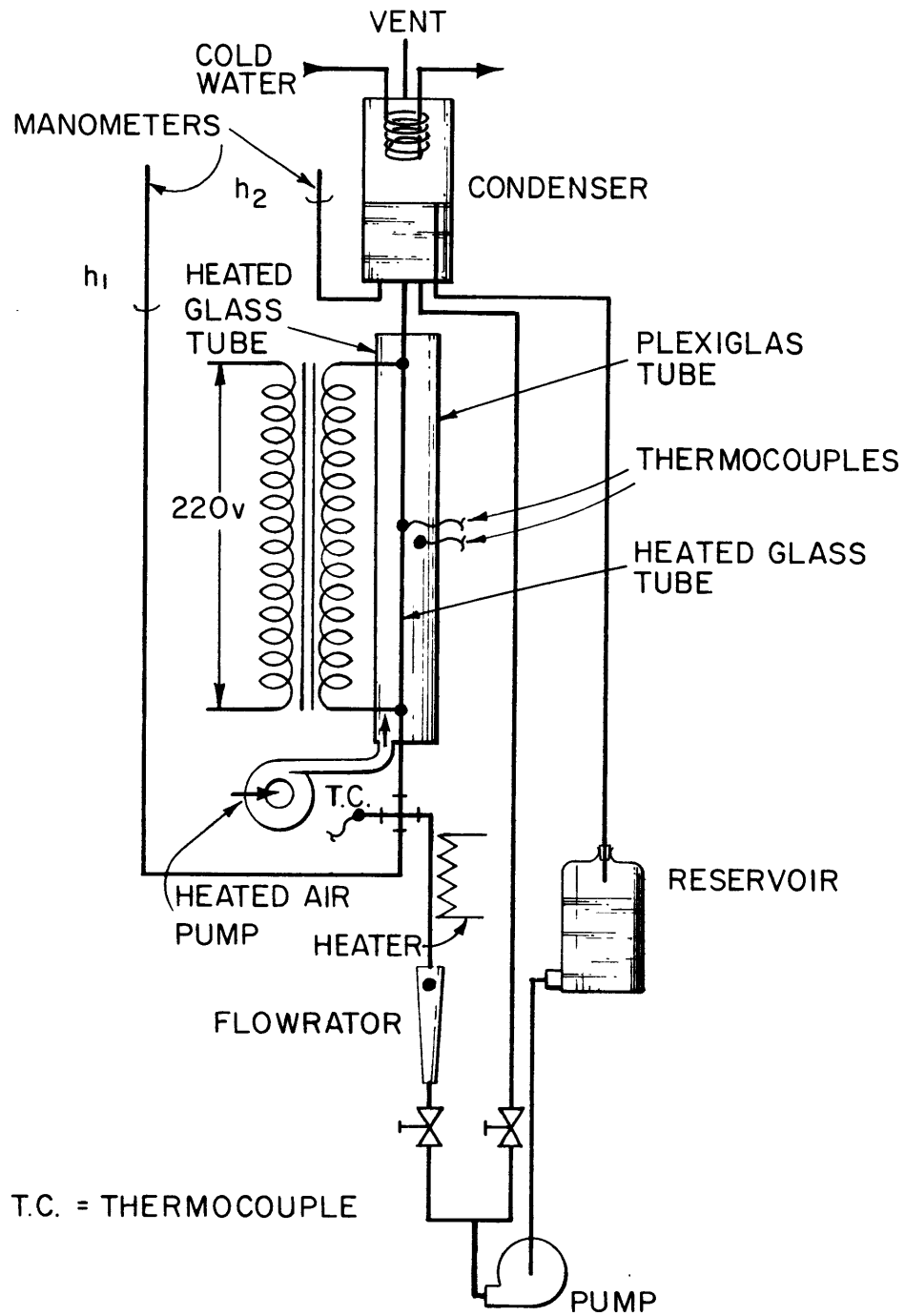


Figure 5

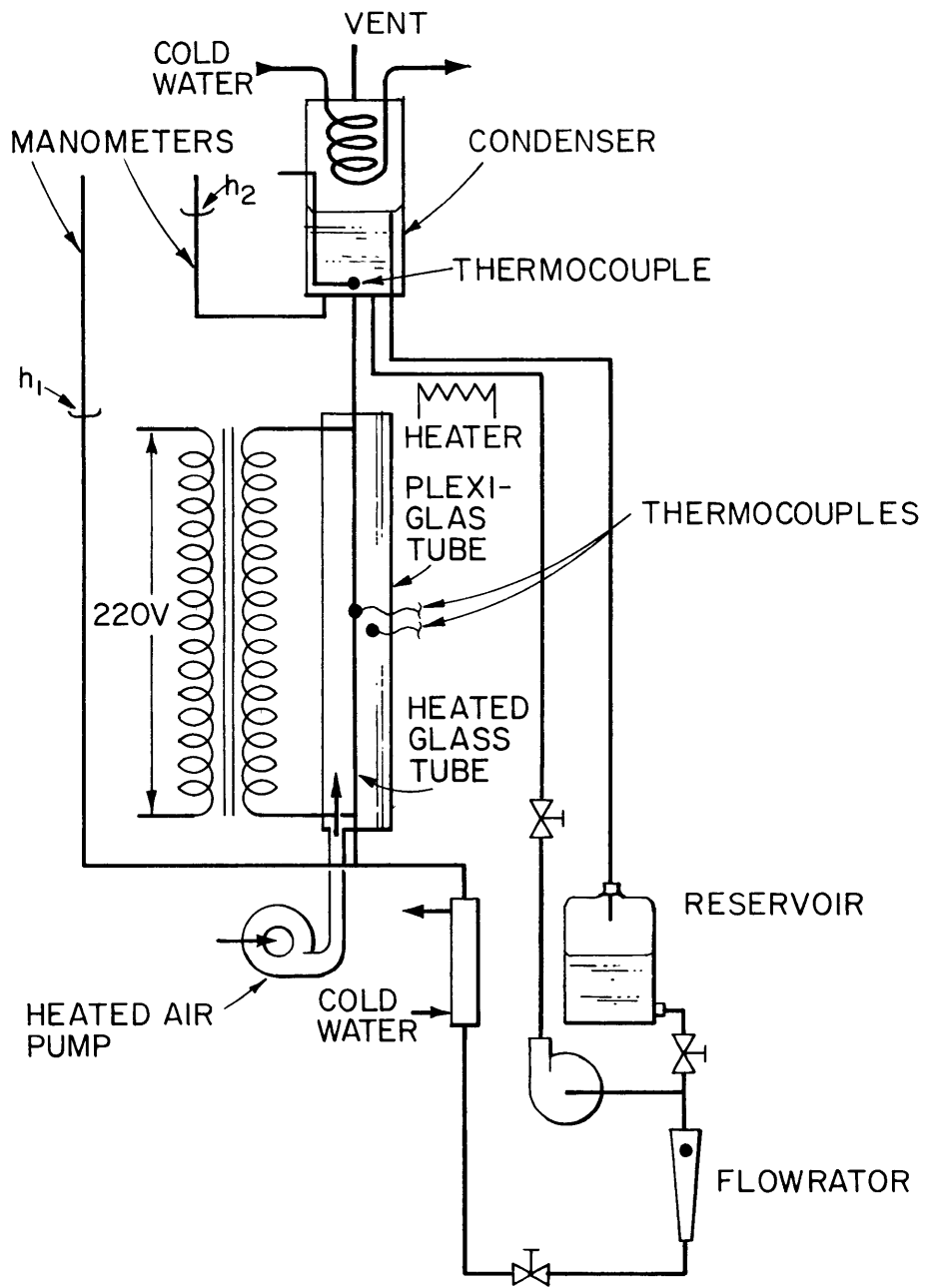


Figure 6

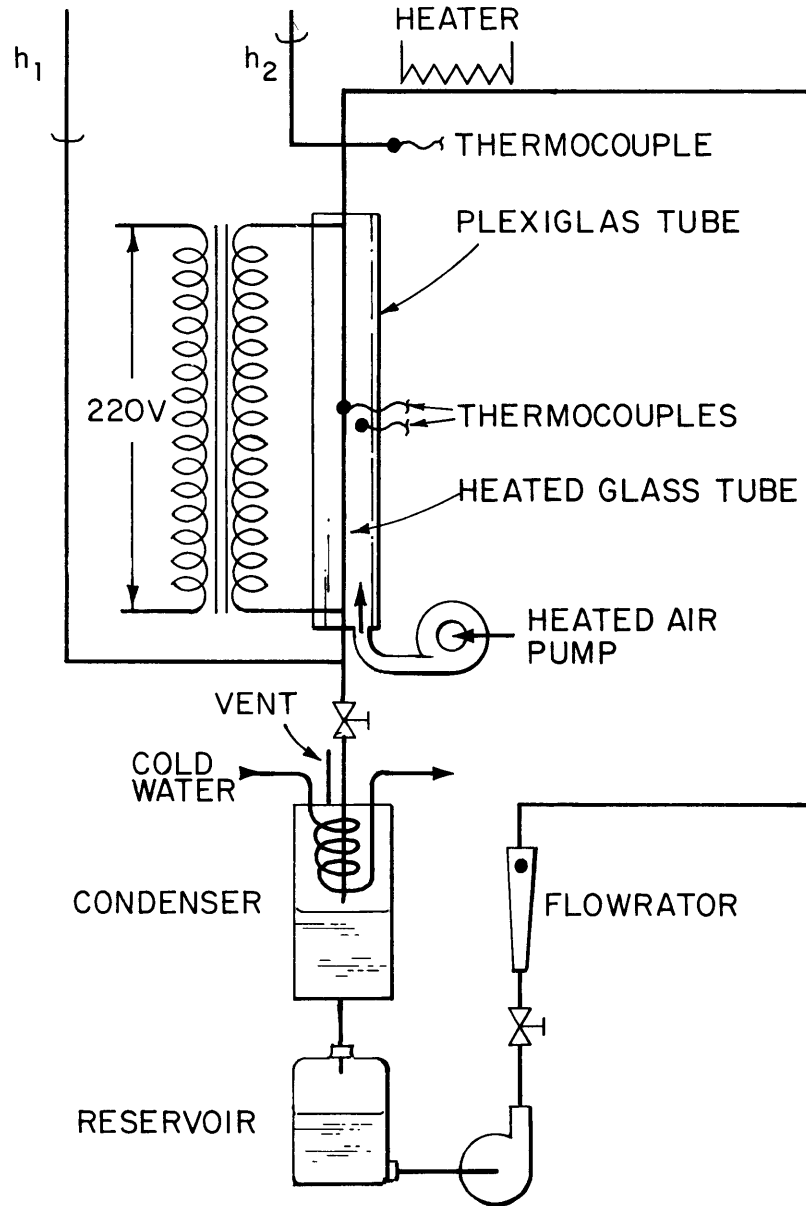


Figure 7

For obtaining the gas down-liquid down data, the pump output was connected to the top of the test section. The test section discharge was then passed into the condenser, as indicated in Fig. 7.

3.2.2. Instrumentation and Auxiliary Equipment

The flow rates to be measured varied from 0 - 1.65 gpm. A Brooks flowrator and a series of Fisher and Porter flowrators were used to accomplish this.

Pre-heating of the Freon was done with an electrical resistance heater which was wrapped around the flow passage in the appropriate place on each test set-up. The amount of heating was controlled by a Variac adjustable transformer which had 115 volts A-C on the primary side.

The A-C electrical power for the test section was obtained from a 220 volt line which was connected to the primary side of a Variac. The output of the Variac was connected to the electrically conducting test section. The voltage and current were monitored to determine the power input to the glass tube. The placement of the electrical connections on the glass tube and the relationship of the heated to the unheated sections of the tube are shown in Fig. 8. Part (a) of this Figure applies to Figs. 5 and 6 and part (b) applies to Fig. 7.

The glass test section was enclosed by a four-inch diameter plexiglas tube into which heated air was introduced. Two thermocouples were used, approximately midway along the heated section, one to measure the tube wall temperature and the other the air temperature. The air temperature was kept near enough to that of the tube wall so that heat losses radially outward from the tube could be neglected. Any deviation from this due to the wall temperature variation along the length was considered negligible. Considering the expected temperature gradient along the tube length and the poor thermal conductivity of glass, longitudinal heat losses were also assumed negligible. Therefore, the assumption was made that the resistance heating of the test section was transferred entirely to the Freon passing through it.

The heated air introduced into the bottom of the plexiglas tube was from a heated air pump. The output temperature of the air from this pump, with a constant current heating element, was varied by a throttle on the air intake.

The thermocouples were constructed from Leeds and Northrup 30-gauge duplex copper-constantan wire. The hot junction of the thermocouple used to measure the wall temperature was separated from the electrical conducting wall by a thin piece of mica and held in place with asbestos cord. A thermocouple, used in each test set-up to measure the inlet temperature of the Freon, was constructed from the same material. An ice bath was used as the cold junction for each thermocouple, but two different potentiometers were used. A Leeds and Northrup potentiometer was used in measuring the inlet Freon temperature. The tube wall and air temperatures were compared with a Rubicon potentiometer.

A cooler, originally expected to act as a condenser for the case of gas and liquid down, was used in the test set-up shown in Fig. 6 to lower the Freon temperature before measuring the flow rate. The pump was unable to draw the liquid down through the test section fast enough to cause the gas to flow downward.

Manometers, as shown in Figs. 5, 6, and 7, contained Freon from the system and were used to determine the pressure drop over the length (L) shown in Fig. 8a and b. The tin oxide coating on the glass tube did not extend over the entire length of the tube. Because of the length added by the compression fittings, it would have been difficult to measure the pressure drop over the heated length only. However, pressure drops over unheated lengths will generally exist when a reactor core or any other array of heated channels is instrumented for pressure drop.

In the test set-ups shown in Figs. 5 and 6 the liquid level in the condenser was maintained at a constant level primarily to facilitate in determining quickly, how the pressure drop was varying. Due to the pressure fluctuations inherent in two-phase flow, it was necessary to place a short piece of constricted rubber tubing in the h_1 manometer line. This increase in the inertance I , ($\rho L/A$), of the manometer line produced satisfactory reduction in the oscillations of the liquid level h_1 .

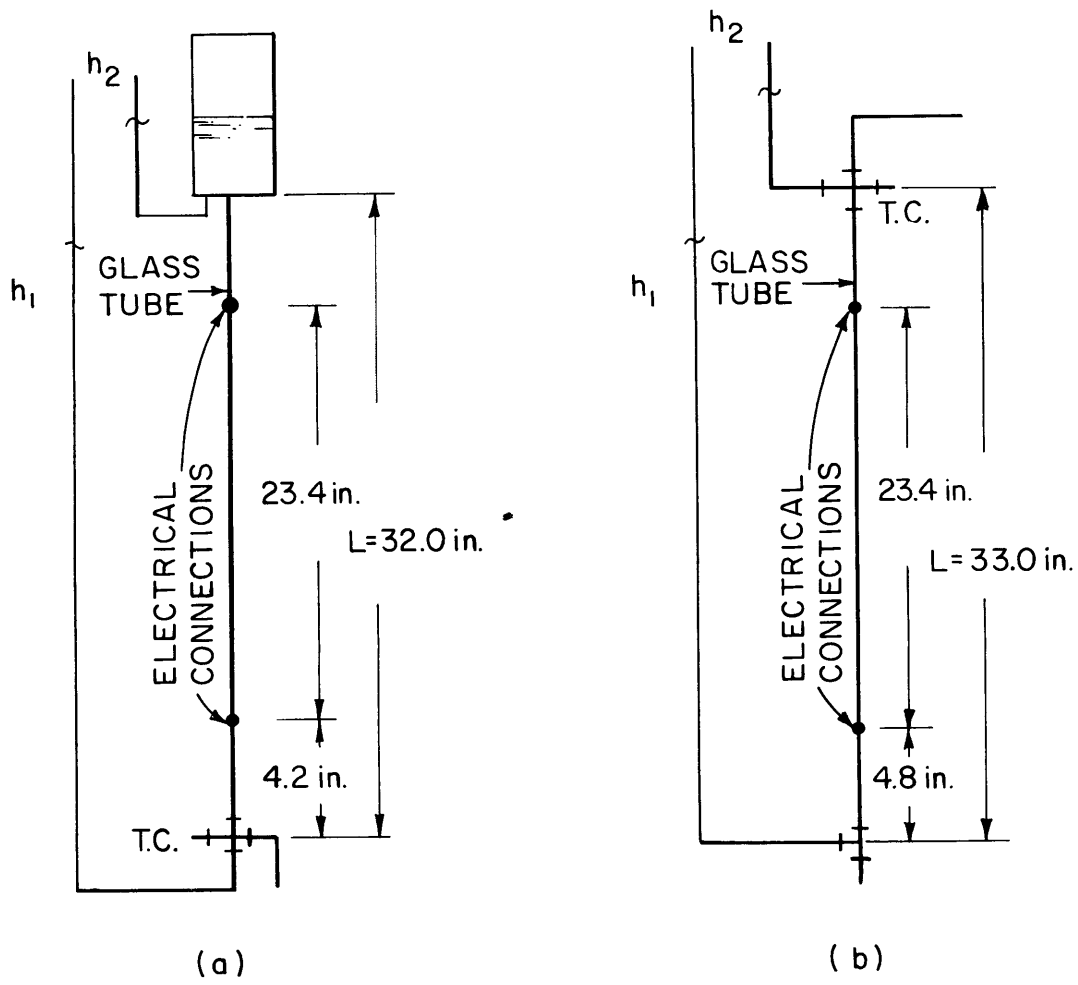


Figure 8

Photographs of the flow regimes were taken with a Polaroid camera. A micro-flash unit was used in conjunction with the camera.

3.3. Experimental Procedure

The test runs for each of the three flow cases were always preceded by a period during which the Freon and the equipment were permitted to warm up. During this period of approximately one hour, both the pre-heater and the test section were used to warm up the Freon.

In taking data for the gas up-liquid up and gas up-liquid down flow cases, the flow rate was initially set at the desired value and held constant throughout the run. The preheater was next adjusted so that the Freon entering the glass tube was within a Fahrenheit degree of the saturation temperature. With the flow rate held constant, the heat flux was increased to the maximum value using the variac. The maximum value of the heat flux was either 5600 BTU/hr-ft.² or a burnout heat flux less than this upper limit of the apparatus. The heat flux upper limit was both a variac limit and a current limit for the tube. For currents of approximately 1.4 amps arcing was found to occur on the tin oxide coating. Data was then taken decreasing the heat flux to discrete values. The data taken for all three flow cases were flow rate, heat flux, pressure drop, checks on the temperatures, and the observed flow regime. The data was taken in the decreasing heat flux direction because it was found that nucleation at lower heat fluxes was obtained in this manner.

The sole purpose in taking data for gas and liquid flowing down was to verify the negative slope of the pressure drop versus flow rate curve. Therefore, the runs were made with constant heat flux, while the flow rate was varied. In general, the runs were made starting at high downward flow rates and decreasing it to discrete lower values. However, some runs were made taking data over the scale of flow rates in both directions. No appreciable difference due to nucleation behavior was noticed.

4. RESULTS AND DISCUSSION

In order to simplify and enhance the general interpretation of the results, the pressure drop has been plotted in terms of $\Delta P_{L,U}/\rho_f g L$, the pressure drop ratio. Also, the superficial liquid velocity ($V_{fs} = Q_f/A$) has been used instead of the flow rate. In all three flow cases, the measured flow rates pertained to liquid entering or leaving the channel in the absence of gas flow. Therefore, the superficial liquid velocity (Q_f/A) becomes the actual velocity. However, for convenience V_{fs} has been carried over from the development of the analytical predictions given in Appendix C.

Pertinent information, with regard to the figures referred to in this chapter, may be found in the Captions, on page iv.

Curves which would be expected to meet or cross the ordinate at $\Delta P_{L,U}/\rho_f g L = 1$, fall short of this since the Freon in the manometer measuring h_1 was cooler than in the channel or the h_2 manometer.

4.1. Pressure Drop Versus Heat Flux Map

The results of the gas up-liquid up and gas up-liquid down experiments plotted on coordinates of ($\Delta P_{L,U}/\rho_f g L$ versus q/Aw) are given in Fig. 9. The zero liquid line ($V_{fs} = 0$), the transition line between these two flow regions, is also shown. Comparison of Fig. 9 with Fig. 4, Sec. 2.5, shows general agreement. In Fig. 4, the constant liquid flow rate curves in the liquid down region are the same shape as those in the liquid up region. However, Fig. 9 shows a change in the curve shape for $V_{fs} < 0.015$ ft/sec. This was due to the fact that this portion of the map corresponds to the counter current annular flow regime. The relation which this flow regime bears to the observed behavior will be discussed in the following sections.

4.2. Flow Regimes and Photographs

In Fig.10, the flow regimes corresponding to Fig. 9 are delineated. The "zero liquid" line ($V_{fs} = 0$) is also shown for reference. For two phase flow in vertical channels with heat transfer, the flow regime will generally change one or more times along the channel length. This, of course, depends on the length of the channel, the heat flux, and other factors. For purposes of having a common reference, the upper most flow regime in the glass test section was chosen for identification. Photographs of some of the regimes are presented in Figs. 16 - 18.

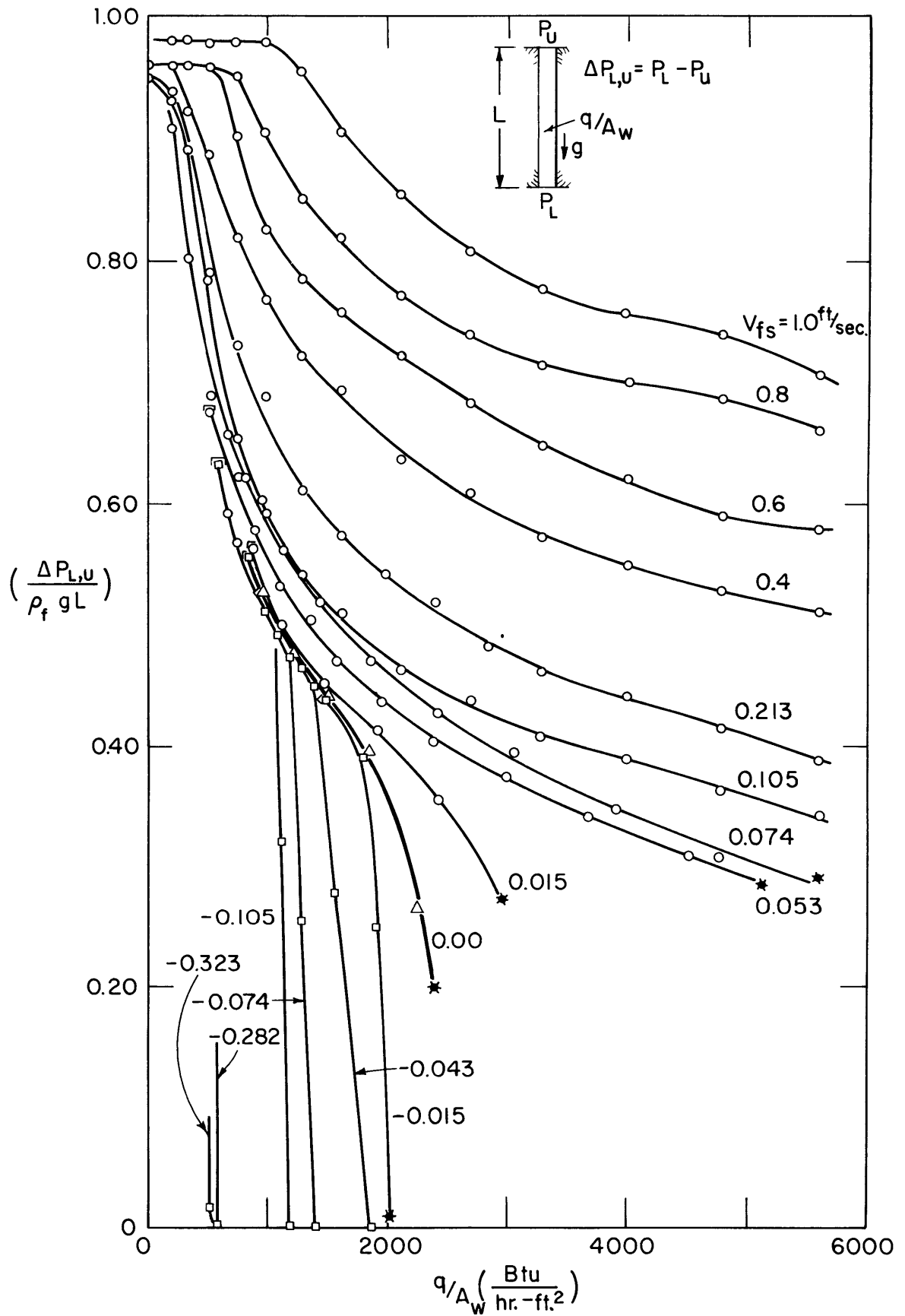


Figure 9

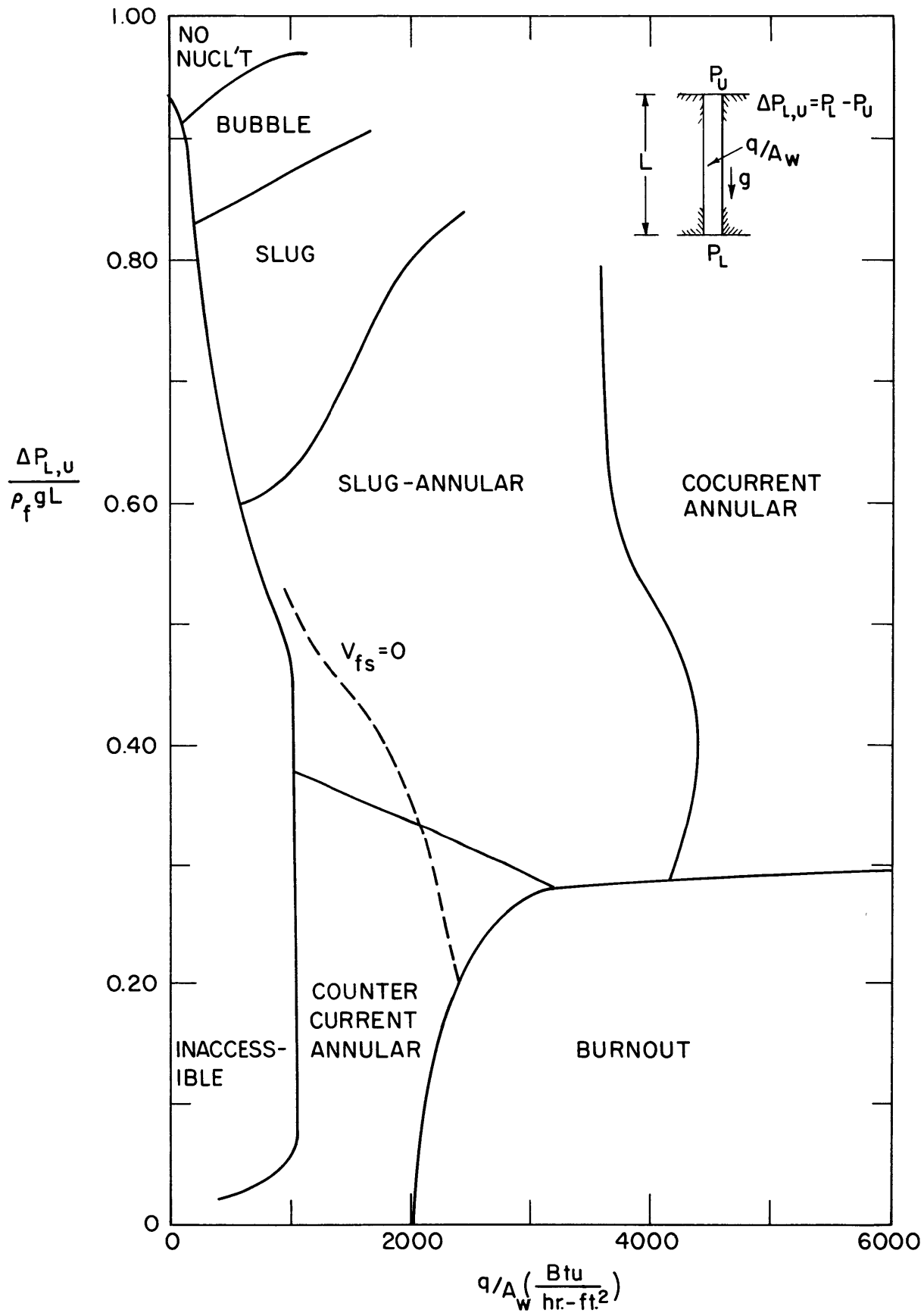


Figure 10

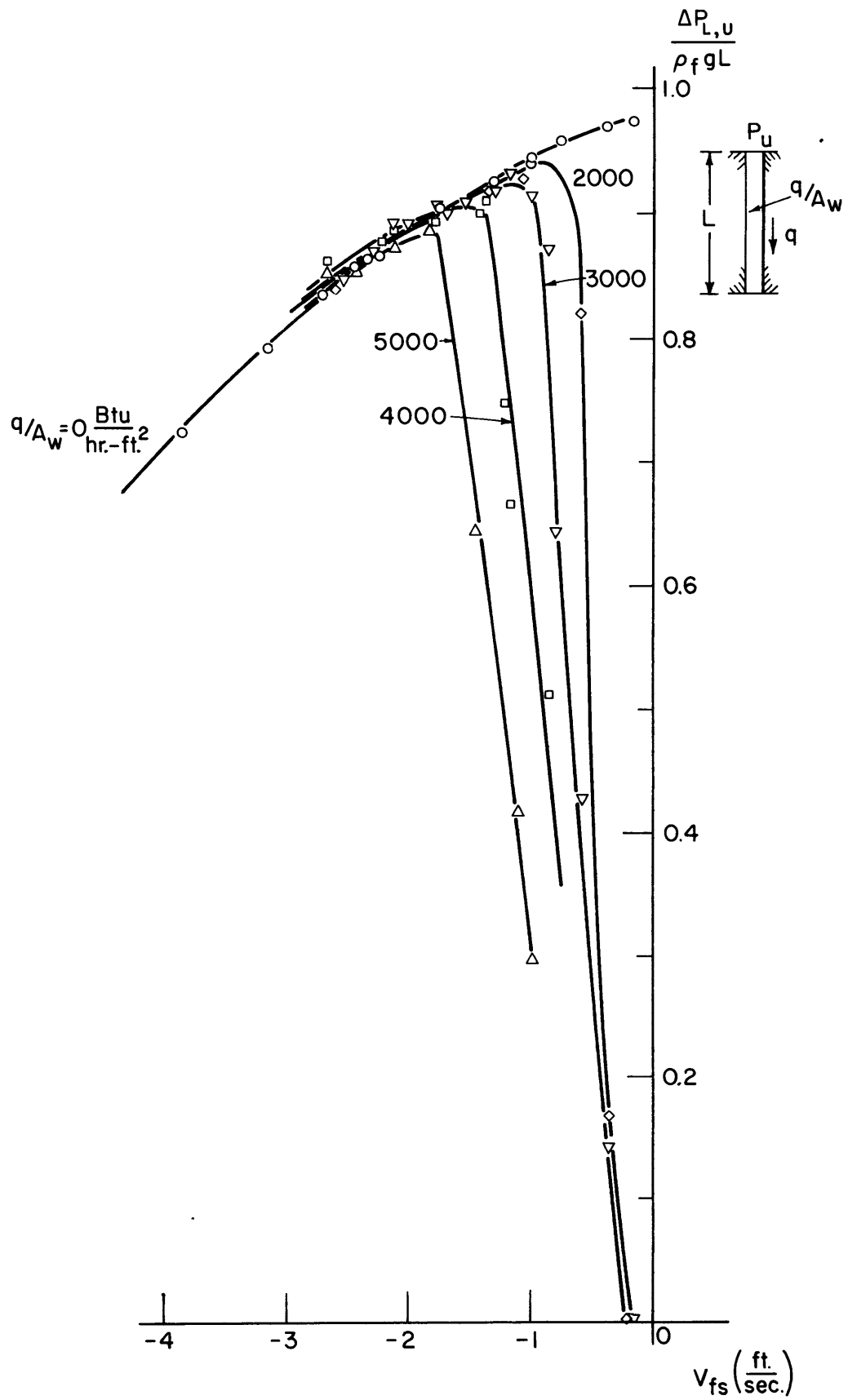
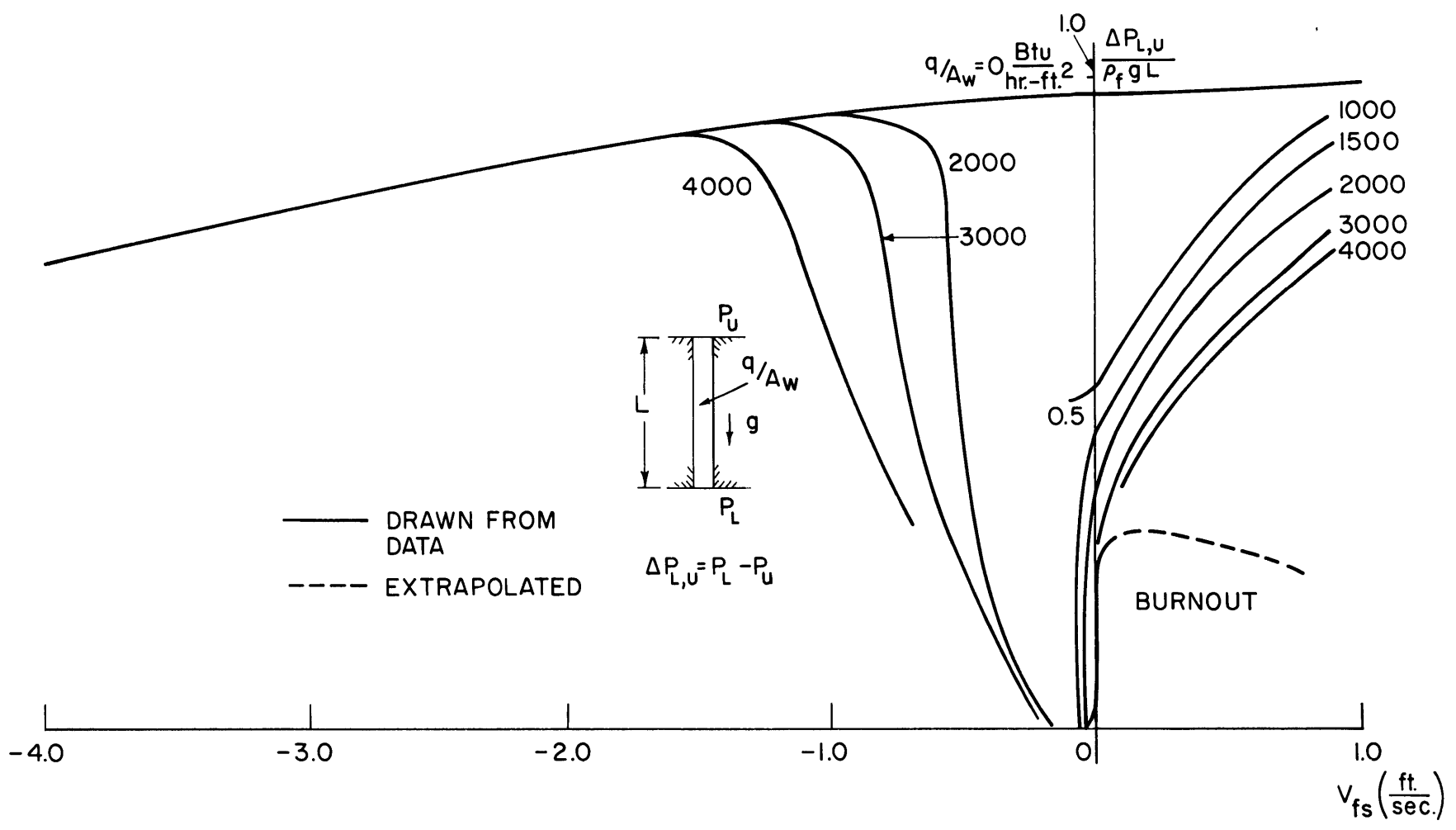


Figure 11

Figure 12



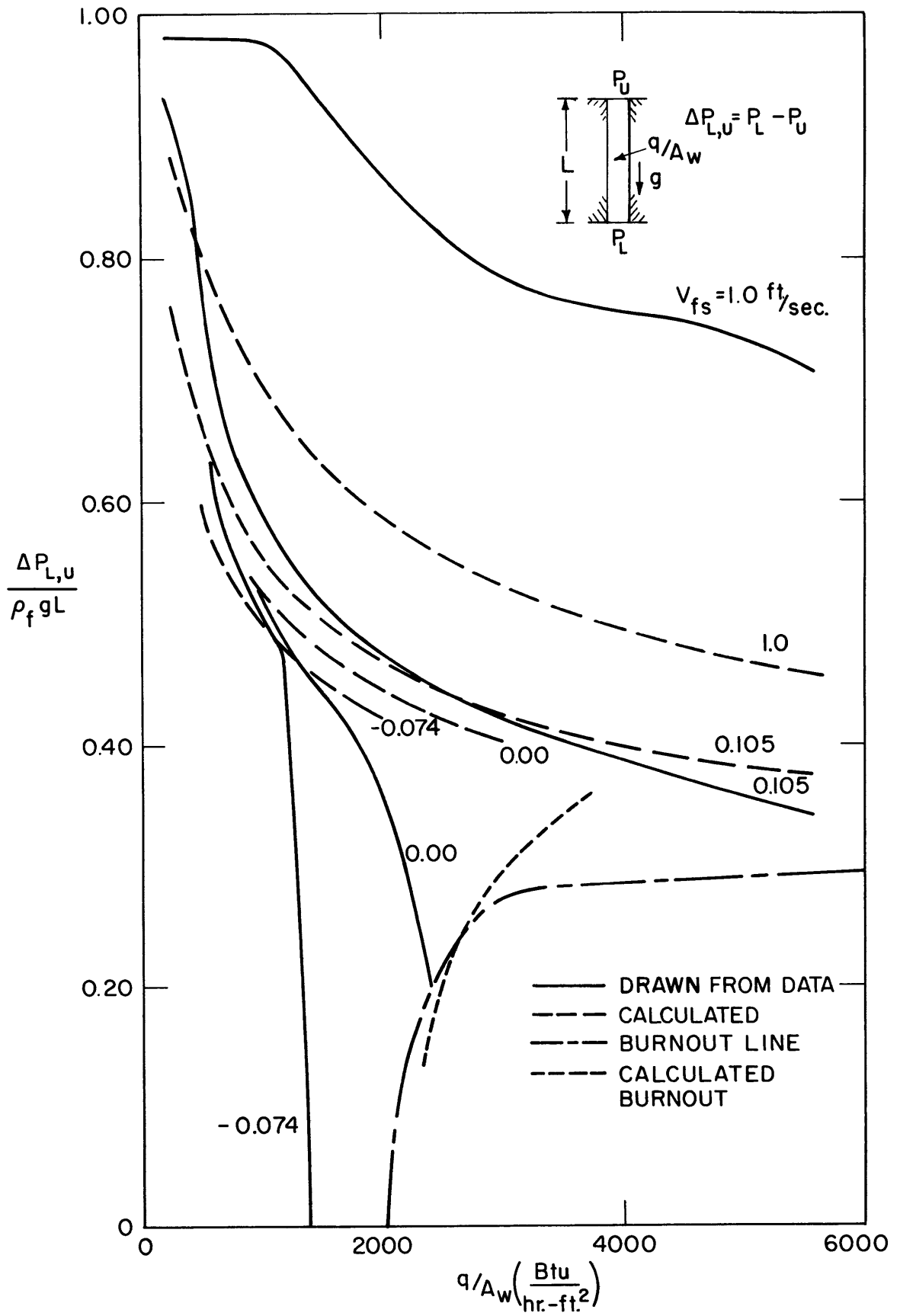


Figure 13

Figure 14

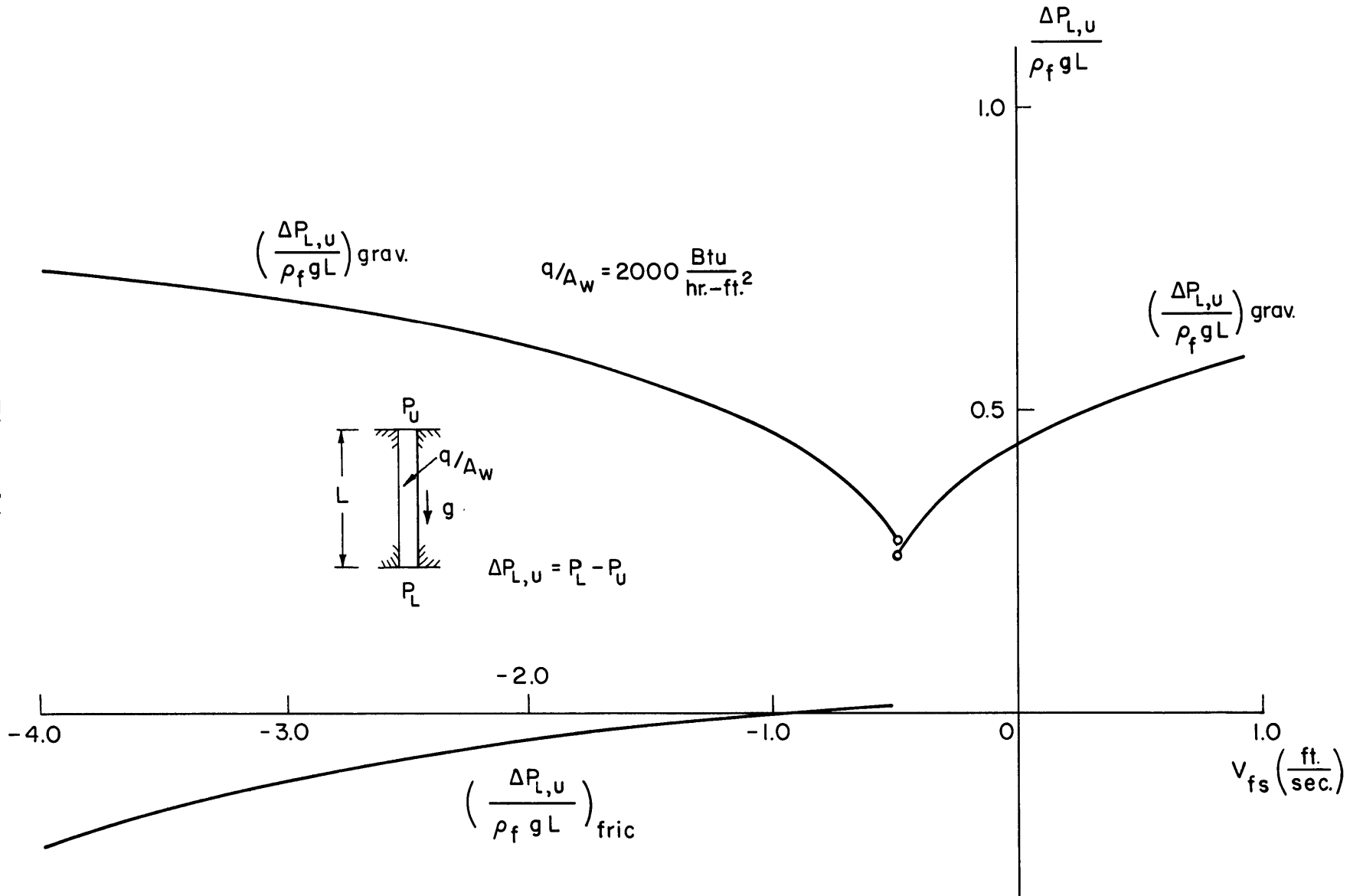
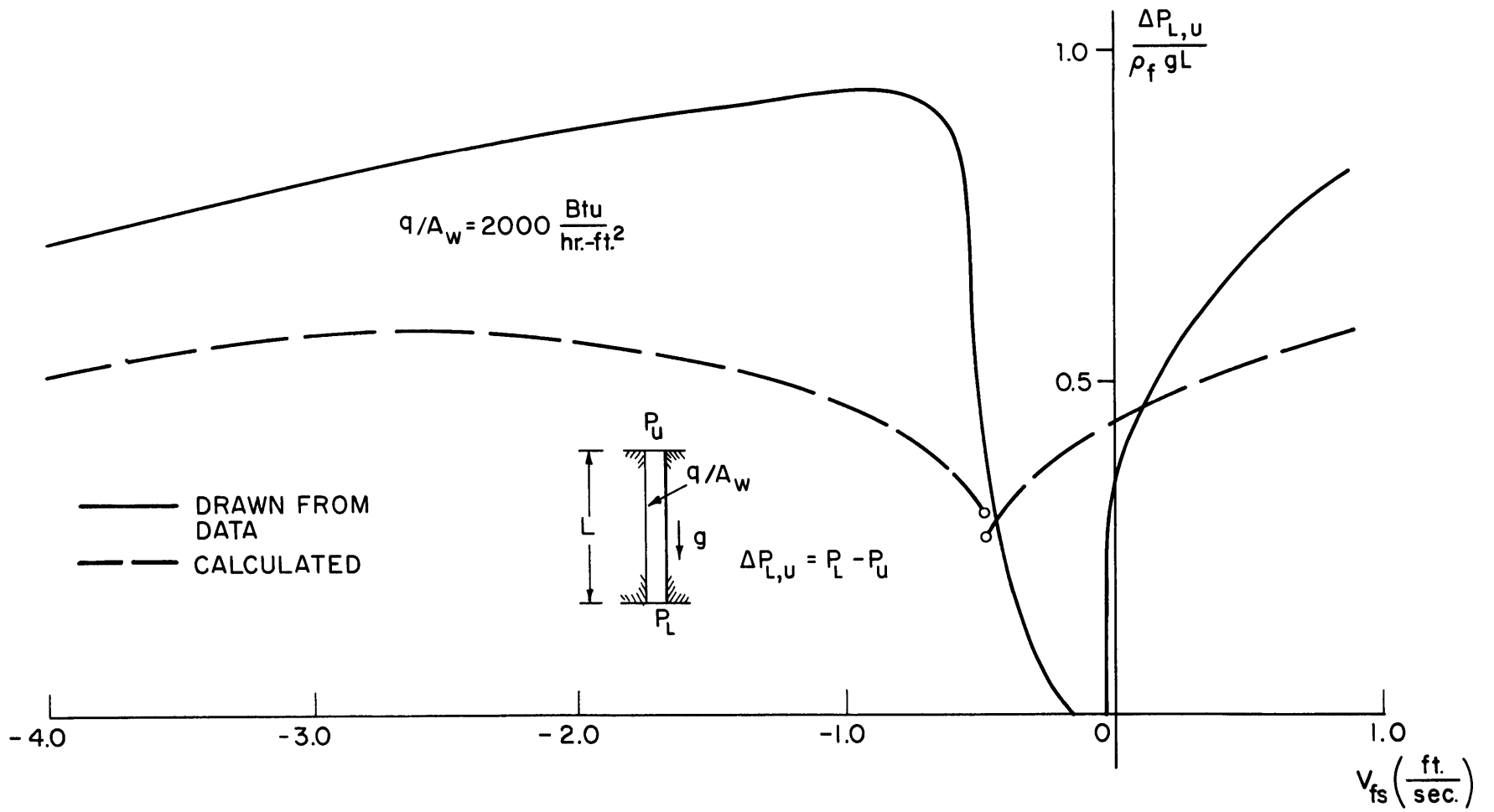


Figure 15



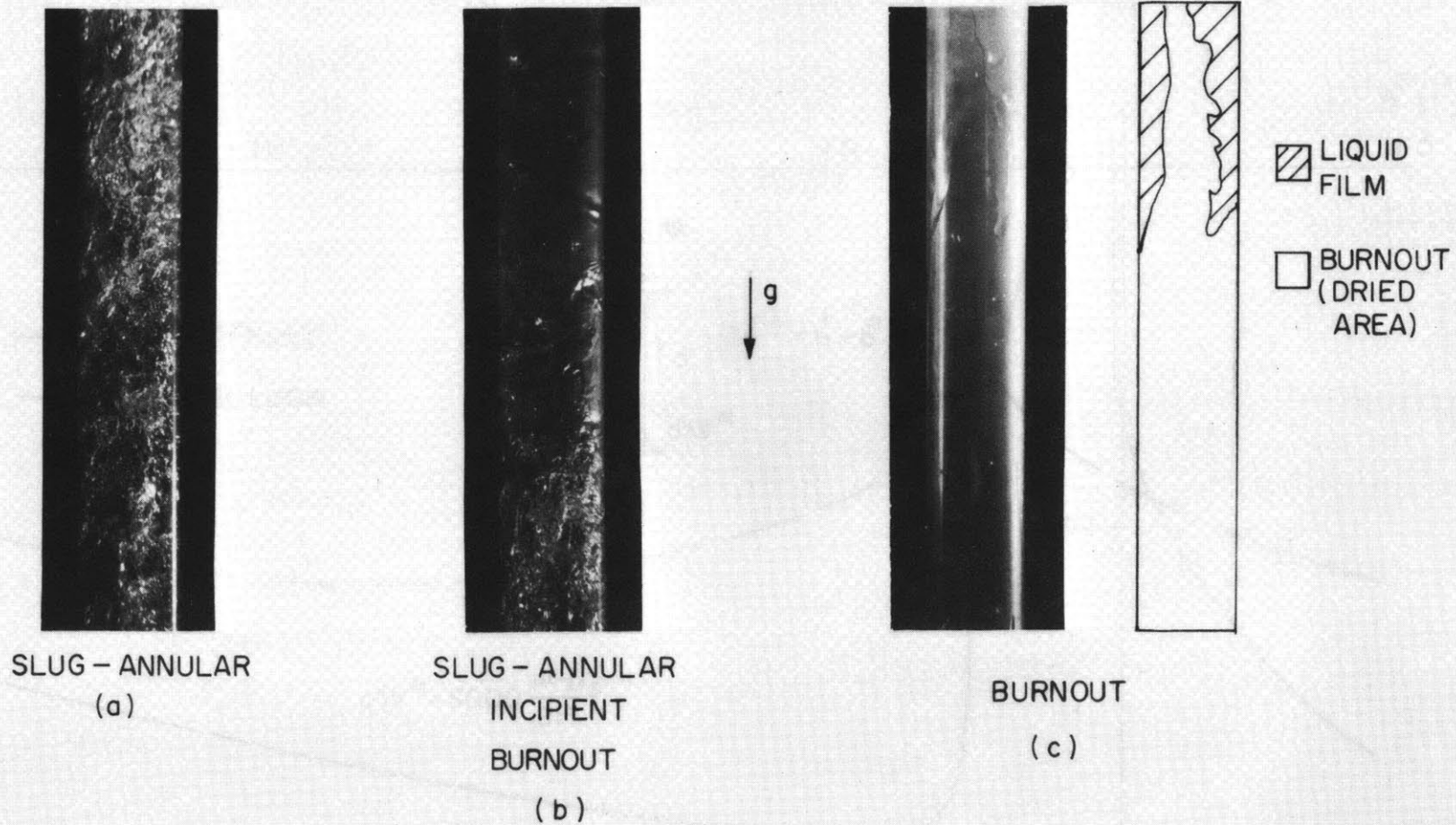
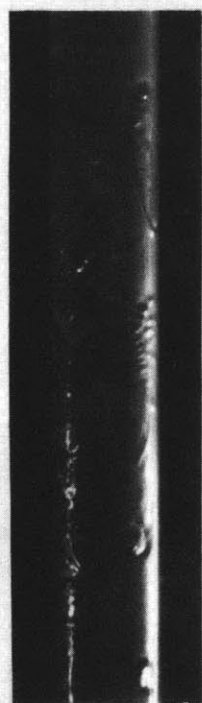
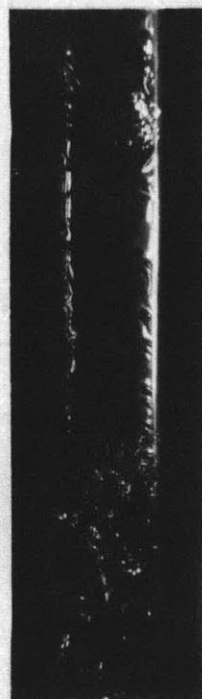


FIGURE 12



COUNTER
CURRENT
ANNULAR
(a)



COUNTER CURRENT
ANNULAR WITH
INTERFACE
(b)

g
↓



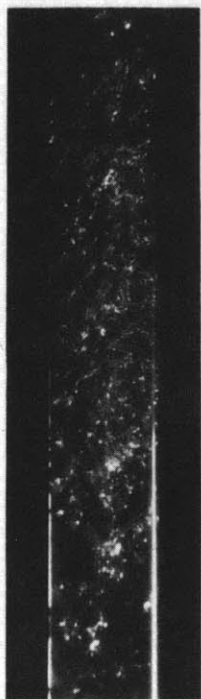
BURNOUT
(c)



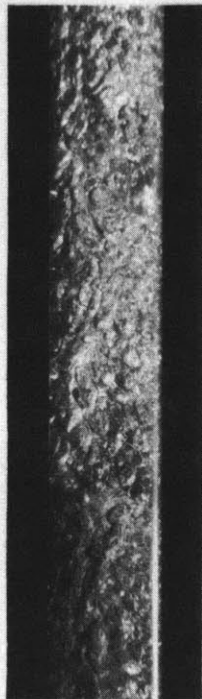
LIQUID
FILM
BURNOUT
(DRIED
AREA)

FIGURE 13

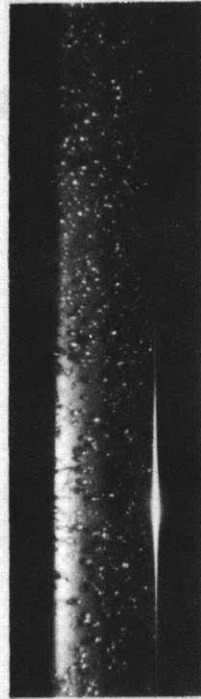
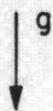
Figure 18



SLUG
(a)



COCURRENT
ANNULAR
(b)



BUBBLY,
GAS AND LIQUID
DOWN
(c)



GAS AND LIQUID
DOWN, INCIPIENT
GAS REVERSAL
(d)

FIGURE 14

The counter current annular regime, referred to in Sec. 4.1, consisted of an annulus of liquid flowing down the channel wall and gas rising in the center, or core. This regime existed from the top of the channel down to a liquid interface with the gas core. Below this interface was a pool of liquid with gas rising through it. Photographs of this regime are shown in Fig. 17a and b. The liquid in the annulus is seen, in Fig. 17 b, to flow into the pool. Since net mass flow may take place in either direction across the flow area of the tube at the interface and at the top of the channel, the feasibility of this regime for liquid entering or leaving at the bottom of the channel is established. This is verified by the combined experimental results shown in Figs. 9 and 10.

The discrepancy between Figs. 9 and 4, which was referred to in Sec. 4.1, is due to the support given to the liquid annulus by the wall and gas shear stresses. This would result in a channel pressure drop which was lower than that anticipated on the basis of the quantity of liquid in the channel. Further verification that the pressure drop in the liquid annulus is negligible along the channel length, can be deduced from the negligible pressure drop through the gas core.

The data for Fig. 9, as previously mentioned in Sec. 3.3, was taken with constant flow rate (or $V_{fs} = \text{constant}$) and decreasing heat flux from the heat flux upper bound. In the gas up-liquid down region of Fig. 9, the burnout point lies on the abscissa for $V_{fs} < -0.015$ ft/sec. This is due to the fact that at the burnout point the gas core and liquid annulus existed over the entire channel length (L). As the heat flux was decreased, the liquid annulus and gas core were present over the entire channel length until the point where the constant V_{fs} curves are shown to depart from the abscissa. The burnout points for these constant V_{fs} curves lie further to the right, on the abscissa, as the magnitude of V_{fs} increases. Therefore, most of the burnout curve of Fig. 4, in the gas up-liquid down region, was found to lie on the abscissa.

In Fig. 9, a random variation in the slope of the curves in the counter current annular region is indicated. This variation in the slope, however, has been found to be a function of the rate at which the heat flux was decreased. For each value of $V_{fs} \leq 0.015$ ft/sec., the curves in Fig. 9 are seen to conform in shape to those for which $V_{fs} > 0.015$ ft/sec., below certain values of heat flux. This value of the heat flux, which varies from curve to curve, will be referred to as $(q/Aw)_c$, for purposes of discussion.

Now, consider the regime in which counter current annular flow exists throughout the channel. The exit liquid flow rate is held constant and the curve lies along the abscissa. If the steady flow continuity equation was assumed to apply, the mass flow rate of liquid entering the top of the channel would decrease along with the heat flux. Under the steady flow assumption, the curve would remain on the abscissa until the corresponding value of $(q/Aw)_c$ was reached. At this point, the curve would rise vertically until it entered the slug-annular regime.

The heat flux $(q/Aw)_c$ is seen to be the minimum heat flux for which the counter current annular regime may exist. However, since the heat flux is decreased at a finite rate, the unsteady term must be added to the continuity equation. The observed result of this was that as the heat flux was decreased, the finite rate of decrease in the flow rate of gas exiting from the tube permitted a momentary increase in the liquid flow rate into the channel. This occurred only as the heat flux approached $(q/Aw)_c$. That is, as the exiting gas flow rate approached the value corresponding to $(q/Aw)_c$. This additional liquid, acquired in the channel during the unsteadiness, resulted in the pool of liquid and gas shown in Fig. 17b. This explains the slope of the curves, in the counter current annular regime, away from the vertical. The slope variations are a function of the rate at which the heat flux was decreased. In general, step decreases in the heat flux of approximately 400 BTU/hr-ft.² were made every ten minutes, in this region.

Some of the curves in Fig. 9 have been terminated due to a nucleation instability. Termination of a curve for this reason is indicated by a bracket. The nucleation instabilities occurred at low heat fluxes and were characterized by erratic nucleation. The discontinuities in vapor generation disturbed the flow and caused the pressure drop to oscillate.

The "no nucleation" region delineated in Fig.10, as well as the nucleation instability, is a function of the channel material. The nucleation instabilities experienced with the glass at low heat fluxes would be decidedly decreased for a metal channel. Experimentation with a metal channel would also reduce the size of the "no nucleation" region.

The region labeled inaccessible in Fig.10 was the result of the flow regime changing from counter current annular to the "no nucleation" region. The flow, or pressure drop, traversed this region on a vertical path without reaching equilibrium.

If the tests resulting in the steep sloping curves of the counter current annular regime had been run with less rapid changes in the heat flux, then this region would also have no data points in it. That is, the counter current annular regime would exist only on the abscissa. Therefore, the region marked counter current annular - excluding the abscissa - would also have been inaccessible if the heat flux had been decreased more smoothly for approximately the same over-all time span.

4.3. Pressure Drop Versus Velocity Map

The data obtained for gas and liquid flowing down is shown in Fig.11. It is seen that a friction and gravity dominated region exists for this flow. Figure 12 shows a pressure drop versus velocity map which includes all of the three flow possibilities. The data from Figs. 9 and 11 were used to construct this map. The shape of a constant heat flux curve in Fig.12 is seen to conform to Fig. 2, in Sec. 2.4.

Let \bar{V}_{fs} be defined in accordance with the definition of \bar{Q} , given in Sec. 2.4, as $\bar{V}_{fs} = \bar{Q}/A$. Figure 12 shows that $(\bar{V}_{fs})_{avg.} \approx -0.12$ ft/sec. Figure 12 also shows that \bar{V}_{fs} occurs in the gravity dominated region. This is evidenced by the shape of the gas down-liquid down curve, the portion of the curve for $V_{fs} < \bar{V}_{fs}$, as discussed in Sec. 2.4.

Figures 18c and d show photographs for $|V_{fs}| > |\bar{V}_{fs}|$ and $V_{fs} \approx \bar{V}_{fs}$, respectively. When V_{fs} was equal to \bar{V}_{fs} a bubble, which had started as shown in Fig. 18d, grew to form the gas core of the co-current annular regime which ensued. This regime, however, is not to be confused

with Fig. 18b which was taken for gas and liquid flowing up. The fact that the liquid flow was being forced in the top of the channel prevented the gas from reversing direction and forming a counter current annular flow pattern.

4.4. Exclusion of Gas and Liquid Flowing Down

In Sec. 2.3, it was shown that the slope of the pressure drop versus flow rate curve for constant heat flux determines the stability of operation of a channel in an array of channels. A positive slope was found to represent stable operation and vice versa.

Figure 12 shows that for gas and liquid flowing down, unstable and stable regions exist. The gravity dominated region is unstable and the friction dominated region is stable.

Considering Fig. 12, a typical curve for constant heat flux is shown in Fig. 19. The curve, which is the operating curve for a channel at a given heat flux, has been separated into parts 1, 2, and 3, as indicated.

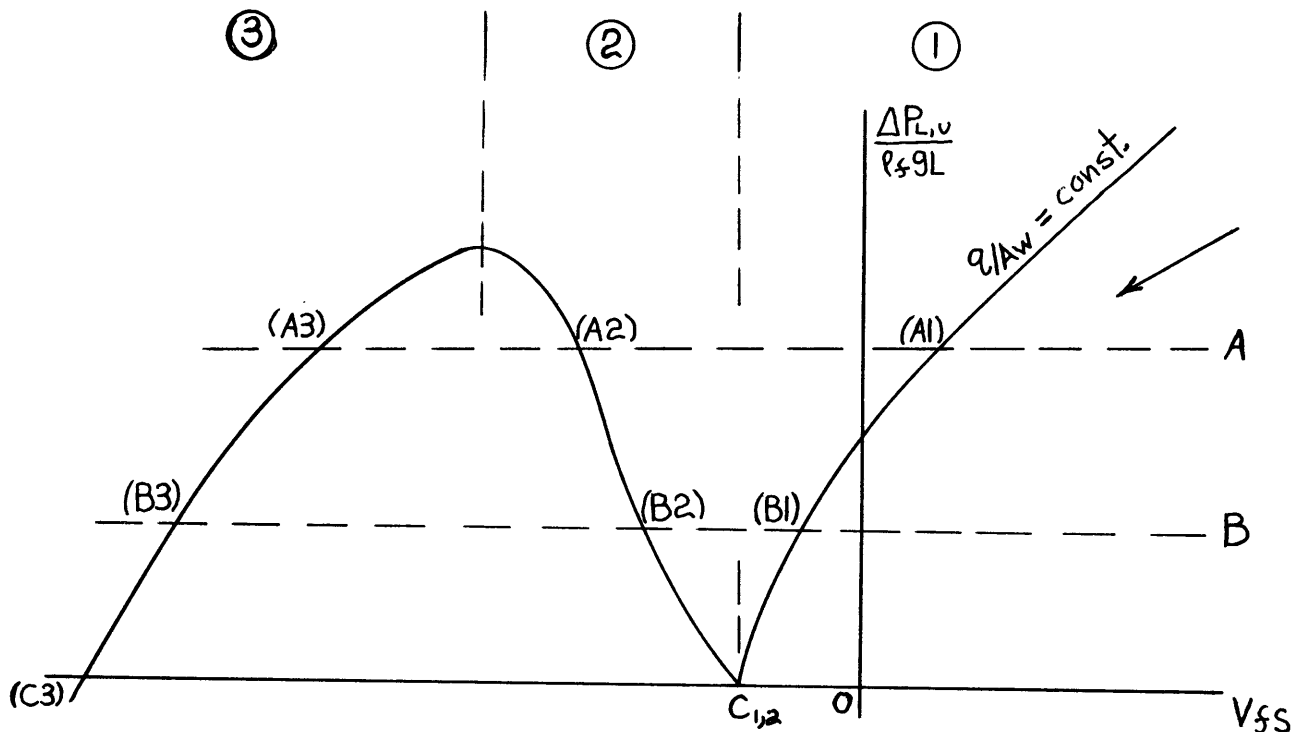


Figure 19

For a channel in an array of channels, part 2 of the curve would be unstable for operation. However, parts 1 and 3 would be stable modes of operation. It is seen that part 3 of the curve is in the gas and liquid down region.

Considering the behavior of a channel in an array of channels, during a "loss of flow" accident, the approach to the region of interest is indicated by the arrow in Fig.19. The horizontal dashed lines A and B represent two possibilities for the pressure drop imposed by the external system; that is, the plenum to plenum pressure drop. If line A represented the system pressure drop, only points A1 and A3 would be stable operating points for the channel. Likewise, for line B, the channel could operate only at points B1 and B3. However, the direction of approach requires that the channel operate on part 1 of the curve. If a flow perturbation occurs while the channel is at a point on part 1 of the curve, the flow will return to that operating point.

If the plenum to plenum pressure drop were zero, the channel would reach point C in Fig.19, a semi-stable point which corresponds with \bar{V}_{fs} . If a perturbation which decreased $|V_{fs}|$ occurred, the flow would return to C_{1,2}. However, if an increase in $|V_{fs}|$ occurred, the channel operating point would proceed to C3 - gas and liquid flowing down. But, point C would never be reached in a "loss of flow" accident. The pressure drop across the array of channels could be zero in only two cases. The first is that all of the channels be burned out. However, since this is to be designed around for all of the channels, it is not a possibility. The second is that counter current annular flow exists throughout each channel. With this flow regime, and no interface in the channel as in Fig. 17b, liquid can enter the channel at the top only. In order to satisfy continuity in the lower plenum, all of the liquid entering the channels, at various flow rates in accordance with the corresponding heat fluxes, must be vaporized at the point where the liquid flow reaches the bottom of the heated channel. Simply from the standpoint of a heat balance, each heat flux distribution over the array of channels at any time during the "loss of flow" accident has the potential for this to occur. In Fig.12, this would be represented by all channels operating at the origin. It is assumed that during the heat flux decay for the array of channels, the vapor generated will condense after passing into

the upper plenum of liquid. Since there is always liquid in the upper plenum, all channels must terminate their trajectories, over the map of Fig. 9, on the ordinate at $\Delta P_{L,U}/\rho_f g L = 1.0$ when the channel heat fluxes have decayed to zero. Throughout the duration of a "loss of flow" accident, all channels must follow trajectories of decreasing heat flux. Also, a common pressure drop and continuity in the lower plenum must be continually satisfied. Figure 9 shows that there is no means by which the trajectories could reach the origin while satisfying these requirements. Therefore, it can be concluded that the case of gas and liquid flowing down will not occur. This assumes that the channels do not interact with one another in such a way so as to cause the pressure drop, $\Delta P_{L,U}$, to fluctuate. If this did occur then one or more of the channels might progress to part 3 of the curve in Fig. 19.

4.5. Analytical Predictions

In Appendix C the acceleration and friction pressure drops are shown to be negligible, in general, for the regions of gas up-liquid up and gas up-liquid down investigated. A calculation procedure for determining the gravity pressure drop, based on determining the average void fraction, is also presented in Appendix C.

Comparisons of the calculated and experimental pressure drops are given in Fig. 13. For $V_{fs} = 0.105$ ft/sec. the prediction is close. For velocities smaller than this, the prediction is high, where the flow enters the counter current annular regime. The prediction assumes that all of the liquid in the channel contributes to the gravity pressure drop. This, however, is far from true in the counter current annular regime. For $V_{fs} = 1.0$ ft/sec. the prediction is low for two reasons. At this velocity, the assumption of an equilibrium heat balance is not accurate. Also, the acceleration pressure drop is not negligible at this entering liquid velocity.

A burnout prediction based on the assumption of flooding as the limiting cause, is also shown in Fig. 13. A flooding criterion presented by Wallis,(3) was used and the procedure is outlined in Appendix D. The prediction is seen to be close in the counter current annular regime, for which it was developed.

A calculation of pressure drop as a function of velocity was also made, corresponding to Fig.12. Friction was accounted for only in the case of gas and liquid down. Figures 14 and 15 show the results and comparison for $q/Aw = 2000 \text{ BTU/hr-ft.}^2$. The discrepancies are large for the reasons previously mentioned. However, the usefulness of the calculation was in the prediction of the nature of the curve before the data was taken.

The calculation procedure developed in Appendix C for the gravity contribution to the pressure drop, which assumes an equilibrium heat balance, is more accurate at higher pressures. A ratio of the superheat liquid enthalpy per unit volume $[\rho_f C_f (T_b - T_s)]$ to the vapor enthalpy per unit volume $(h_{fg} \rho_g)$ is a decreasing function of pressure. In a report by Griffith,(4) this point is brought out and supporting experimental data is presented.

5. CONCLUSIONS

1. Three different flow combinations are possible in a single heated channel at low velocity when both vapor and liquid are present and the pressure difference across the channel is fixed.

- a. Both phases can flow up.
- b. The liquid can go down and the gas phase go up.
- c. Both phases can flow down.

2. In an array of a large number of channels, the possibility (a) above, is stable (the pressure drop versus flow rate curve has a positive slope). Possibility (b) is also stable. Possibility (c) is unstable until the downward liquid velocity is so large that the friction pressure drop is the governing term in the pressure drop equation. This means very little vapor if any is likely to be dumped into the bottom plenum.

3. A method of tracing out the reactor pressure drop versus time curve is proposed based on a mass balance on the lower plenum.

4. Analytical methods for predicting the void are inadequate, at least at low pressures, because of substantial departures from equilibrium. These occur due to erratic nucleation and superheat in the liquid.

5. It is not yet clear whether the friction dominated gas down-liquid down flow case is ever attainable in a large number of parallel heated channels.

APPENDIX A. STABILITY ANALYSIS

In this analysis the effect of a flow perturbation, or excursion, upon the stability of the flow in a single heated channel with constant pressure drop is examined. The heat flux is also held constant and the model becomes that of a channel operating in an array of channels.

In Fig. 15 the pressure drop ratio versus velocity curves from the data and calculation procedure of Appendix C are presented for constant heat flux. From either of these curves and the coordinates on which they are plotted, it can be deduced that the general slope of the pressure drop versus flow rate curve will be the same. In the single channel experiments the liquid flow rate measured was the entering liquid flow rate in all cases except gas up-liquid down. However, the gas to liquid density ratio of Freon 113 and heat fluxes worked with are such that the liquid flow rate entering and leaving are approximately equal. Therefore, Fig. 15 may be considered representative of $(\Delta P_{L,U}$ versus Q_{in}), where Q_{in} denotes the liquid flow rate entering the channel. Also, small portions of the curve may be represented in generalized slope intercept form as,

$$\Delta P_{L,U} = \left[R(Q_{in}) + K(Q_{in}) \right] Q_{in} + B(Q_{in}) \quad (21)$$

The terms $R(Q_{in})$ and $K(Q_{in})$, which comprise the slope; account for the friction and gravity pressure drop contributions, respectively. For the case of gas and liquid flowing down the slope $\left[R(Q_{in}) + K(Q_{in}) \right]$ is positive in the "friction dominated" region and negative in the "gravity dominated" region.

For purposes of investigating the dynamic response to a flow perturbation for a channel operating at any point on the curve of Fig. 15, the pressure drop may be expressed as

$$\Delta P_{L,U} = I(Q_{in}) \frac{dQ_{in}}{dt} + \left[R(Q_{in}) + K(Q_{in}) \right] Q_{in} + B(Q_{in}) \quad (22)$$

The coefficient I , $(\rho L/A)$, is the inertance of the gas and liquid mixture in the channel. If the heat flux is constant, the mass of vapor generated per unit of time is also constant. However, the density of the mixture in the channel will be a function of Q_{in} .

If a small perturbation in the entering flow rate, ΔQ_{in} , is to be considered for a channel operating at a particular point on the characteristic curve of Fig. 15 then Eq. (22) may be linearized. That is,

$$\Delta P_{L,U} = I \frac{dQ_{in}}{dt} + (R + K) Q_{in} + B \quad (23)$$

As previously mentioned, the stability is to be examined for constant pressure drop with a flow perturbation superimposed on some initial flow rate. That is,

$$\Delta P_{L,U} = \left[\Delta P_{L,U} \right]_c \quad (24)$$

Before the perturbation is introduced,

$$\frac{dQ_{in}}{dt} = 0 \quad (25)$$

Therefore,

$$\left[\Delta P_{L,U} \right]_c = (R + K)Q_{in} + B$$

or

$$(Q_{in})_i = \frac{\left[\Delta P_{L,U} \right]_c - B}{(R + K)} \quad (26)$$

From Eqs. (23) and (24),

$$\frac{dQ_{in}}{dt} + \frac{R + K}{I} Q_{in} = \frac{\left[\Delta P_{L,U} \right]_c - B}{I} \quad (27)$$

Performing a Laplace transform on both sides of Eq. (27)

$$S\bar{Q}_{in}(s) - Q_{in}(0^+) + \frac{R+K}{I} \bar{Q}_{in}(s) = \frac{[\Delta P_{L,U}]_c - B}{I} \frac{1}{S}$$

At time zero plus, the step input perturbation ΔQ_{in} is introduced such that

$$Q_{in}(0^+) = (Q_{in})_i + \Delta Q_{in}$$

$$\therefore \left[S + \frac{R+K}{I} \right] \bar{Q}_{in}(s) = \frac{[\Delta P_{L,U}]_c - B}{I} \frac{1}{S} + (Q_{in})_i + \Delta Q_{in}$$

or

$$\bar{Q}_{in}(s) = \frac{[\Delta P_{L,U}]_c - B}{I} \frac{1}{R+K} \frac{\frac{R+K}{I}}{S \left[S + \frac{R+K}{I} \right]} + \frac{(Q_{in})_i + \Delta Q_{in}}{\left[S + \frac{R+K}{I} \right]}$$

Since,

$$\frac{[\Delta P_{L,U}]_c - B}{R+K} = (Q_{in})_i \quad (26)$$

$$\bar{Q}_{in}(s) = (Q_{in})_i \frac{\frac{R+K}{I}}{S \left[S + \frac{R+K}{I} \right]} + \frac{(Q_{in})_i + \Delta Q_{in}}{\left[S + \frac{R+K}{I} \right]} \quad (28)$$

$$\bar{Q}_{in}(s) = \frac{(Q_{in})_i}{S} + \frac{\Delta Q_{in}}{\left[S + \frac{R+K}{I} \right]}$$

Therefore, taking the inverse Laplace transformation of both sides of Eq. (28)

$$Q_{in}(t) = (Q_{in})_i + \Delta Q_{in} e^{-(R+K/I)t}$$

or,

$$Q_{in}(t) = (Q_{in})_i + \Delta Q_{in} e^{-t/\tau} \quad (29)$$

where

$$\tau = \frac{I}{R + K} \quad (30)$$

It can be seen that for stability it is necessary to have $\tau \geq 0$. Since the inertance I , $(\rho L/A)$, is always positive, the criterion becomes $R + K > 0$. The term $(R + K)$ is the slope at a point on the pressure drop versus flow rate curve. From Fig. 15, and the previous discussion, it is seen that the "gravity dominated" portion of the gas and liquid flowing down region, is unstable.

Suggestions for the analytical evaluation of R and K are made in the section on pressure drop, Appendix C. If data has been taken, it is suggested that the slope be evaluated from the data directly for substitution into Eq. (19).

APPENDIX B. VOID FRACTION

An expression, due to Griffith and Wallis (5), for the void fraction in slug flow is,

$$\alpha = \frac{Q_g}{(1 + K_2)(Q_f + Q_g) + K_1 K_3 \sqrt{gDA}} \quad (31)$$

Or, in terms of the superficial gas and liquid velocities,

$$\alpha = \frac{V_{gs}}{(1 + K_2)(V_{fs} + V_{gs}) + K_1 K_3 \sqrt{gD}} \quad (32)$$

These equations apply to the three flow cases, gas up-liquid up, gas up-liquid down, and gas down-liquid down when the proper signs for the velocities, or flow rates, are used. The upwards direction is taken as positive.

In the latter expression for α , the denominator represents the velocity of a bubble with respect to the channel wall. The downward liquid velocity for which a bubble is held stationary is found by setting the denominator equal to zero. This velocity will be symbolized by \bar{V}_{fs} .

$$(1 + K_2)(\bar{V}_{fs} + V_{gs}) + K_1 K_3 \sqrt{gD} = 0 \quad (33)$$

But, when this occurs, $V_{gs} = 0$. Therefore,

$$\bar{V}_{fs} = \frac{-K_1 K_3 \sqrt{gD}}{(1 + K_2)} \quad (34)$$

In the case of a heated channel this bubble would be expected to grow in both directions and cause counter or co-current annular flow to ensue. Which regime followed this occurrence would depend upon the end conditions. That is, upon whether the liquid was being drawn out the bottom by suction or forced in the top, respectively. For a heated section, from reference (5), $K_1 = 0.34$, $K_2 = 0.2$ and $K_3 = 1.6$. Therefore, from Eq. (34)

$$\bar{V}_{fs} = \frac{-(0.34)(1.6)\sqrt{\left(32.2 \frac{\text{ft.}}{\text{sec.}^2}\right)\left(\frac{0.419 \text{ in.}}{12 \text{ in./ft.}}\right)}}{1.2}$$

$$\therefore \bar{V}_{fs} = -0.482 \text{ ft./sec.}$$

For an unheated section, $K_1 = 0.34$, $K_2 = 0.2$ and $K_3 = 1.0$.

APPENDIX C. PRESSURE DROP ANALYSIS

As discussed in Sec. 2.1, the two phase pressure drop is considered to be the sum of the acceleration, friction and gravity contributions. That is,

$$\Delta P = (\Delta P)_{\text{acc.}} + (\Delta P)_{\text{fric.}} + (\Delta P)_{\text{grav.}} \quad (35)$$

These individual contributions, and the magnitude of their importance in this investigation, will be considered here.

1. Acceleration Pressure Drop

$$(\Delta P)_{\text{acc.}} A = \frac{D}{Dt} (mV) = \iiint_{\text{c.v.}} \frac{\partial}{\partial t} (\rho V) d\mathcal{U} + \oint_{\text{c.s.}} \rho V(V \hat{n}) ds \quad (36)$$

The first term accounts for the unsteadiness of the flow in the control volume. The second term takes into account the change in the momentum flux over the surface of the control volume. In two phase flow both unsteadiness and slip between the phases exists. However, the results of Andeen and Griffith (6) show that the experimental two-phase pressure drop in a channel is most accurately computed as

$$(\Delta P)_{\text{acc.}} = \left[(\rho V^2)_{\text{out}} - (\rho V^2)_{\text{in}} \right] \quad (37)$$

using a homogeneous model. From continuity, assuming steady flow

$$\rho_i V_i = \rho_o V_o; \quad V_o = V_i \frac{\rho_i}{\rho_o} = V_i \frac{U_o}{U_i} \quad (38)$$

but,

$$U_i = U_f$$

$$\therefore V_o = V_i \frac{U_o}{U_f}$$

Now, from Eqs. (37) and (38)

$$\begin{aligned}
 (\Delta P)_{acc.} &= \left[\rho_o V_o^2 - \rho_i V_i^2 \right] = \frac{1}{U_o} \left(V_i \frac{U_o}{U_f} \right)^2 - \frac{1}{U_f} V_i^2 \\
 &= \frac{V_i^2}{U_f} \left[\frac{U_o}{U_f} - 1 \right]
 \end{aligned}$$

Now

$$U_o = U_f + X U_{fg} \quad (39)$$

or,

$$\frac{U_o}{U_f} = 1 + X \frac{U_{fg}}{U_f}$$

where

$$X = \frac{W_g}{W_f + W_g} \quad (40)$$

$$\therefore (\Delta P)_{acc.} = \frac{V_i^2}{U_f} \left(X \frac{U_{fg}}{U_f} \right) = \left(\frac{V_i}{U_f} \right)^2 U_{fg} X = (\rho_f V_i)^2 \left(\frac{1}{\rho_g} - \frac{1}{\rho_f} \right) X$$

$$= (\rho_f V_i)^2 \left(\frac{\rho_f - \rho_g}{\rho_f \rho_g} \right) X = V_i^2 \frac{\rho_f}{\rho_g} (\rho_f - \rho_g) X$$

Since no vapor enters the control volume at the inlet

$$W_f + W_g = \rho_f V_i A \quad (41)$$

At the outlet, assuming a heat balance

$$W_g = \frac{q}{h_{fg}} \quad (42)$$

Therefore, the flowing quality at the outlet is

$$X = \frac{q}{\rho_f V_i h_{fg} A} \quad (43)$$

Therefore,

$$(\Delta P)_{acc.} = \left(\frac{\rho_f}{\rho_g} - 1 \right) \frac{V_i q}{h_{fg} A} = \left(\frac{\rho_f}{\rho_g} - 1 \right) \frac{4 V_i L \left(\frac{q}{A w} \right)}{h_{fg} D} \quad (44)$$

or,

$$\frac{(\Delta P)_{acc.}}{\rho_f g L} = \left(\frac{\rho_f}{\rho_g} - 1 \right) \frac{4 V_i \frac{q}{A w}}{\rho_f g h_{fg} D} \quad (45)$$

$$\rho_f (118^\circ F) = 94.26 \text{ lbm/ft.}^3$$

$$\rho_g (118^\circ F) = 0.461 \text{ lbm/ft.}^3$$

$$\frac{\rho_f}{\rho_g} = 205$$

$$h_{fg} = 63.12 \text{ BTU/lbm}; \quad D = 0.035 \text{ ft.}$$

From Eq. (45)

$$\begin{aligned} \frac{(\Delta P)_{acc.}}{\rho_f g L} &= \frac{(204) 4 V_i \frac{q}{A w}}{(94.26 \text{ lbm/ft.}^3)(32.2 \text{ ft/sec.}^2)(63.12 \text{ BTU/lbm})(0.035 \text{ ft.})(3600 \text{ sec./hr.})} \\ &= 3.38 \times 10^{-5} \frac{\text{ft-sec-hr}}{\text{BTU}} \left(V_i \frac{q}{A w} \right) \end{aligned}$$

an average value of $(V_i q / Aw)$ for the gas up-liquid up and gas up-liquid down experiments was

$$\left(V_i \frac{q}{Aw} \right) = \left(0.3 \frac{\text{ft}}{\text{sec.}} \right) \left(3000 \frac{\text{BTU}}{\text{hr-ft.}^2} \right) = 900 \frac{\text{BTU}}{\text{ft-sec-hr}}$$

Therefore,

$$\left(\frac{(\Delta P)_{\text{acc.}}}{\rho_f g L} \right)_{\text{avg.}} = 0.0304$$

so that in general $(\Delta P)_{\text{acc.}}$ is negligible in this investigation.

2. Friction Pressure Drop

An investigation by Govier, Radford and Dunn(1) gives the effect of air and water rates on pressure drop for vertical flow of these components. For an entering liquid velocity of 0.873 ft/sec. the frictional unit pressure drop (in feet of water per foot) was found to be negligible up to $Q_g / Q_f = 13$. The particular experiment was run in a pipe 22.88 ft long with a 1.025 in. I. D. In this investigation the gas flow rate varies over the channel length and for comparison purposes the average at the highest heat flux $(q / Aw) = 5600$ BTU/hr-ft.² is used. From a heat balance,

$$\Delta V_{gs} = \frac{Q_{go}}{A} = \frac{q}{\rho_g A h_{fg}} \quad (46)$$

$$\frac{1}{2} \Delta V_{gs} = 0.001065 \left(\frac{q}{Aw} \right) = 5.97 \frac{\text{ft}}{\text{sec}}$$

Therefore,

$$\frac{(Q_g)_{\text{avg.}}}{Q_f} = \frac{\frac{1}{2} \Delta V_{gs} A}{V_{fs} A} = \frac{5.97 \frac{\text{ft}}{\text{sec}}}{0.873 \frac{\text{ft}}{\text{sec}}} = 6.83$$

On this basis the frictional pressure drop for the cases of gas up-liquid up and gas up-liquid down, for which $V_{fs} \leq 1$ ft/sec, is considered to be negligible.

For the case of gas and liquid down the velocities are so large that friction may not be neglected. For this flow case when the liquid entering velocity was approximately equal to or greater than one foot per second, the void fraction was small. This is indicated in Fig. 18c. For this reason the frictional pressure drop was calculated on the basis of a single phase (liquid) model. Therefore, the standard frictional and sudden contraction and expansion pressure drop equations were used. The friction pressure drop over the heated length, taking into account the acceleration of the liquid due to vapor generation, was accounted for as follows

$$(\Delta P_{L_2})_{\text{fric.}} = \int_0^{L_2} \frac{4f(\rho V^2)}{D^2} dy \quad (47)$$

where

$$V = V_{fsi} + \Delta V_{gs} \frac{Y}{L} \quad (48)$$

The heated length (L_2) is defined in part 3 of this appendix. From continuity, assuming steady flow,

$$\rho V = \rho_f V_{fsi} \quad (49)$$

Therefore, Eq. (47) becomes

$$(\Delta P_{L_2})_{\text{fric.}} = \frac{4f(\rho_f V_{fsi})}{D^2} \int_0^{L_2} \left(V_{fsi} + \Delta V_{gs} \frac{Y}{L} \right) dy \quad (50)$$

$$= 2f \rho_f V_{fsi} \left(\frac{L_2}{D} \right) \int_0^1 (V_{fsi} + \Delta V_{gs} Y^*) dy^* \quad (51)$$

for $Y^* = Y/L_2$

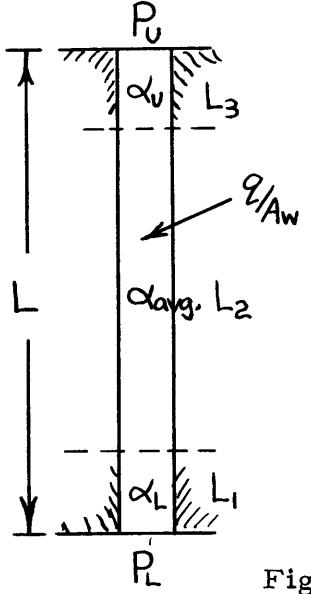
therefore,

$$(\Delta P_{L_2})_{\text{fric.}} = 2f \left(\frac{L_2}{D} \right) \rho_f V_{fsi}^2 \left(1 + \frac{\Delta V_{gs}}{2 V_{fsi}} \right) \quad (52)$$

In this equation, $Q_i = V_{fsi}A$. The friction contribution for the unheated section, and the contraction losses can be totaled to get the slope of ΔP versus Q_i . The slope of this curve is R . Figure 14 shows a portion of this curve in terms of $\Delta P_{L,U}/\rho_f gL$ versus V_{fs} .

3. Gravity Pressure Drop

On the basis of the void fraction (α) the gravity pressure drop may be computed as follows:



$$(\Delta P)_{\text{grav.}} = P_L - P_U = (1 - \alpha_L) \rho_f g L_1 + (1 - \alpha_a) \rho_f g L_2 + (1 - \alpha_U) \rho_f g L_3 \quad (53)$$

and

$$\left(\frac{\Delta P_{L,U}}{\rho_f g L} \right)_{\text{grav.}} = \frac{(1 - \alpha_L) L_1 + (1 - \alpha_a) L_2 + (1 - \alpha_U) L_3}{L} \quad (54)$$

Fig. C-1

In Fig. C-1, the length L_1 and L_3 are unheated while L_2 is heated. The void fraction α_{avg} is the average void fraction over the heated length (L_2), as shown in Fig. C-1. According to which flow case is being considered, either α_L or α_U will be zero since gas does not enter the channel. From Appendix B,

$$\alpha = \frac{V_{gs}}{(1 + K_2)(V_{fs} + V_{gs}) + K_1 K_3 \sqrt{gD}} \quad (31)$$

or,

$$\alpha = \frac{V_{gs}}{C_o(V_{fs} + V_{gs}) + \bar{V}_g} \quad (56)$$

for

$$C_o = 1 + K_2 \quad \text{and} \quad \bar{V}_g = K_1 K_3 \sqrt{gD}$$

In order to determine the average void fraction (α_{avg}), it is necessary to integrate a generalized expression for α , over the heated length. The expression for the average void fraction is the same for all three flow cases. Only gas and liquid flowing up will be considered here. By definition

$$(a) \quad V_{fsi} = \frac{W_{fi}}{\rho_f A} \quad (b) \quad V_{fs} = \frac{W_f}{\rho_f A} \quad (c) \quad V_{gs} = \frac{W_g}{\rho_g A} \quad (57)$$

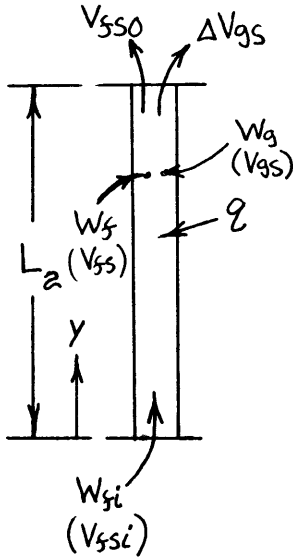


Fig. C-2

from a heat balance,

$$\Delta V_{gs} = \frac{\frac{q}{h_{fg}}}{\rho_g A} \quad (58)$$

$$W_g = \rho_g \Delta V_{gs} A \left(\frac{Y}{L_2} \right) \quad (59)$$

From Eq. (57C)

$$V_{gs} = \frac{W_g}{\rho_g A} = \Delta V_{gs} \left(\frac{Y}{L_2} \right) \quad (60)$$

From continuity,

$$W_f = W_{fi} - \rho_g \Delta V_{gs} A \left(\frac{Y}{L_2} \right) \quad (61)$$

$$V_{fs} = \frac{W_f}{\rho_f A} = V_{fsi} - \frac{\rho_g}{\rho_f} \Delta V_{gs} \left(\frac{Y}{L_2} \right) \quad (62)$$

From Eqs. (60) and (62)

$$V_{fs} + V_{gs} = V_{fsi} + \left(1 - \frac{\rho_g}{\rho_f} \right) \Delta V_{gs} \left(\frac{Y}{L_2} \right) \quad (63)$$

Now,

$$\left(1 - \frac{\rho_g}{\rho_f} \right) = \left(1 - \frac{0.461}{94.26} \right) = 0.995 \approx 1 \quad (64)$$

$$\therefore V_{fs} + V_{gs} = V_{fsi} + \Delta V_{gs} \left(\frac{Y}{L_2} \right)$$

Substitution of Eq. (64) into Eq. (56) yields

$$a = \frac{\Delta V_{gs} \left(\frac{Y}{L_2} \right)}{C_o \left[V_{fsi} + \Delta V_{gs} \left(\frac{Y}{L_2} \right) \right] + \bar{V}_g} \quad (65)$$

The average void fraction over the heated is

$$a_{avg.} = \frac{1}{L_2} \int_0^{L_2} a \, dy \quad (66)$$

or

$$a_{avg.} = \int_0^1 a \, dy^* \quad (67)$$

for

$$Y^* = \frac{Y}{L_2} \quad (68)$$

After combining Eqs. (68) and Eq. (65) and substituting the result into Eq. (67)

$$\alpha_{avg.} = \int_0^1 \frac{\Delta V_{gs} Y^*}{C_o \left[V_{fsi} + \Delta V_{gs} Y^+ \right] + \bar{V}_g} dy^* \quad (69)$$

Integrating,

$$\alpha_{avg.} = \frac{1}{C_o} - \frac{(C_o V_{fsi} + \bar{V}_g)}{C_o^2 \Delta V_{gs}} \ln \left[\frac{C_o (V_{fsi} + \Delta V_{gs}) + \bar{V}_g}{C_o V_{fsi} + \bar{V}_g} \right] \quad (70)$$

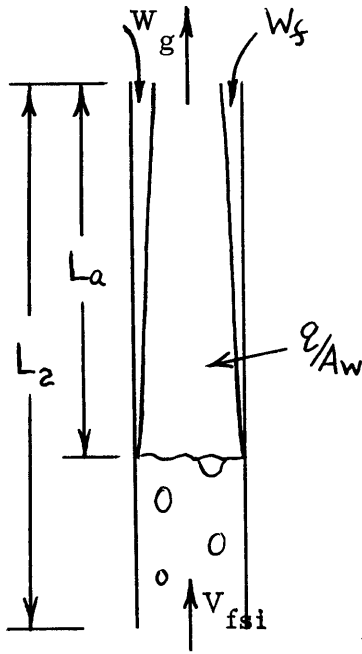
The variables are, V_{fsi} and ΔV_{gs} which is a function of the heat flux. For gas up-liquid up, $\alpha_L = 0$ and From Eq. (56)

$$\alpha_U = \frac{\Delta V_{gs}}{C_o \left[V_{fsi} + \Delta V_{gs} \right] + \bar{V}_g} \quad (71)$$

Equations (70) and (71) along with the relation $Q_i = V_{fsi} A$ can be used to develop a curve of $(\Delta P)_{grav.}$ versus Q_i . The shape of this curve is K. This curve is shown in Fig. 14 in terms of $\Delta P_{L,U} / \rho_f g L$ versus V_{fs} .

APPENDIX D. BURNOUT ANALYSIS

A burnout prediction is developed here on the basis of the flooding phenomena as the limiting cause of the burnout. Flooding occurs in counter current annular flow when the gas velocity is such as to cause the appearance of waves on the liquid film. This disrupts the liquid flow in the annulus and is a possible cause of burnout. In reference to Fig.D-1, it is assumed for incipient burnout that



$$W_f = W_g \left(\frac{L_a}{L_2} \right) \quad (72)$$

From a heat balance,

$$W_g = \frac{q}{h_{fg}} \quad (73)$$

Therefore,

$$W_f = \frac{q}{h_{fg}} \left(\frac{L_a}{L_2} \right) \quad (74)$$

Fig. D-1

Using Eqs. (73) and (74),

$$V_{gs} = \frac{W_g}{\rho_g A} = \frac{q}{\rho_g h_{fg} A} \quad (75)$$

and

$$V_{fs} = \frac{W_f}{\rho_f A} = \frac{q}{\rho_f h_{fg} A} \left(\frac{L_a}{L_2} \right) \quad (76)$$

Therefore,

$$\frac{V_{fs}}{V_{gs}} = \frac{\rho_g}{\rho_f} \left(\frac{L_a}{L_2} \right) \quad (77)$$

A flooding criterion by Wallis (3) which correlates experimental data is,

$$\sqrt{V_{fs}^*} + \sqrt{V_{gs}^*} = 0.725 \quad (78)$$

where by definition,

$$V_{fs}^* = \frac{V_{fs}}{\left[gD \left(\frac{\rho_f - \rho_g}{\rho_f} \right) \right]^{1/2}} \quad (79)$$

and

$$V_{gs}^* = \frac{V_{gs}}{\left[gD \left(\frac{\rho_f - \rho_g}{\rho_g} \right) \right]^{1/2}} \quad (80)$$

Combining Eqs. (79) and (80) gives

$$\frac{V_{fs}}{V_{gs}} = \frac{V_{fs}^*}{V_{gs}^*} \left(\frac{\rho_g}{\rho_f} \right)^{1/2} \quad (81)$$

Eq. (77) may be expressed in terms of V_{fs}^* and V_{gs}^* by combining it with Eq. (81) which gives,

$$\frac{V_{fs}^*}{V_{gs}^*} = \left(\frac{\rho_g}{\rho_f} \right)^{1/2} \left(\frac{L_a}{L_2} \right) \quad (82)$$

The results of combining Wallis's flooding criterion, Eq. (78) with Eq. (82) is

$$\sqrt{V_{gs}^*} \left[\frac{\left(\frac{L_a}{L_2} \right)^{1/4}}{\left(\frac{\rho_f}{\rho_g} \right)} + 1 \right] = 0.725 \quad (83)$$

If a value of L_a is chosen, a corresponding value of ΔV_{gs} is determined since V_{gs}^* is a function of ΔV_{gs} . Since, ΔV_{gs} is a function of q/Aw , a corresponding value of heat flux is also determined.

The pressure drop over the length (L_a) is negligibly small, and the over-all value of

$$\left(\frac{\Delta P_{L,U}}{\rho_f g L} \right) = \left(\frac{\Delta P_{L,U}}{\rho_f g L} \right)_{\text{grav.}} \quad (84)$$

may be determined after solving for α_{avg} as outlined in Appendix C, part 3. In the region of interest, $-0.015 < V_{fs} < +0.03$. Therefore, it is assumed that $V_{fsi} \approx 0$ in determining α_{avg} . From this analysis a burnout line may be plotted on the coordinates ($\Delta P_{L,U}/\rho_f g L$ versus q/Aw).

APPENDIX E. TEST SECTION SPECIFICATIONS

Glass Tube 13 mm O.D. x 30 inches - Corning Glassware.

0.419 inches I.D. - Tin oxide external coating over
27 inches, starting 1-1/2 inches from
the ends.

Measured resistance, 100 ohm/ft.

Highest amperage passed, 1.44 amps.

APPENDIX F. SOME PHYSICAL PROPERTIES - DU PONT FREON 113
(CCl₂F - CClF₂)

Boiling Point at 1 atm (°F)	117.63*
Density, Liquid at 77°F (lbm/ft ³)	97.69
Density, Saturated Vapor at Boiling Point (lbm/ft ³)	0.461
Specific Heat, Liquid at 77°F (BTU/lbm °F)	0.707
Heat of Vaporization at Boiling Point (BTU/lmb)	63.12
Viscosity, Liquid (centipoise)	0.66
Surface Tension at 77°F (dynes/cm)	23

*

Properties are from DuPont Freon Technical Bulletin B-2

$$\rho \left(\frac{\text{lbm}}{\text{ft}^3} \right) = 103.55 - 0.07126T - 0.0000636 T^2; \quad T(^{\circ}\text{F})$$

BIBLIOGRAPHY

1. Govier, G.W., Radford, B.A., and Dunn, J.S.C., "The Upwards Vertical Flow of Air Water Mixtures I - Effect of Air and Water-Rates on Flow Pattern, Holdup and Pressure Drop", Can.J.Chem. Engr., 35 No. 2, 1957, pp. 58-78.
2. Maulbetsch, J.S., and Griffith, P., "A Study of System - Induced Instabilities in Forced-Convection Flows with Sub-cooled Boiling," Report No. 5382-35, Dept. of Mech. Engr., Mass. Inst. of Tech., April 15, 1965.
3. Wallis, G.B., "Flooding Velocities for Air and Water in Vertical Tubes," AEEW-R-123, Atomic Energy Establishment, Winfrith, England, 1961.
4. Griffith, P., "The Prediction of Low Quality Boiling Voids," Report No. 77673-23, Dept. of Mech. Engr., Mass. Inst. of Tech., January 1963.
5. Griffith, P., and Wallis, G.B., "Two-Phase Slug Flow", J. Heat Transfer Trans. ASME, Series C, 84, 1961.
6. Andeen, G.B., and Griffith, P., "The Momentum Flux in Two-Phase Flow", Report No. 4547-38, Dept. of Mech. Engr., Mass. Inst. of Tech., AEC Code: Report MIT-3496-1, October 1965.